Late Carboniferous dextral transpressional reactivation of the crustal-scale Walls Boundary Fault, Shetland: the role of pre-existing structures and lithological heterogeneities

Timothy B. Armitage[1]*, Lee M. Watts[2], Robert E. Holdsworth[1] and Robin A. Strachan[3]

[1] Department of Earth Sciences, Durham University, Durham DH1 3LE, UK
[2] Brunei Shell Petroleum, Seria Head Office, Jalan Utara, Seria, KB3534, Sultanate of Brunei
[3] School of the Environment, Geography and Geoscience, University of Portsmouth, Portsmouth PO1 3QL, UK
TBA, 0000-0001-5652-1698; REH, 0000-0002-3467-835X
* Correspondence: timothy.b.armitage@durham.ac.uk

Abstract: The Walls Boundary Fault in Shetland, Scotland, formed during the Ordovician–Devonian Caledonian orogeny and underwent dextral reactivation in the Late Carboniferous. In a well-exposed section at Ollaberry, westerly verging, gently plunging regional folds in the Neoproterozoic Queyfirth Group on the western side of the Walls Boundary Fault are overprinted by faults and steeply plunging Z-shaped brittle–ductile folds that indicate contemporaneous right-lateral and top-to-the-west reverse displacement. East of the Walls Boundary Fault, the Early Silurian Graven granodiorite complex exhibits fault-parallel fractures with Riedel, P and conjugate shears indicating north–south-striking dextral deformation and an additional contemporaneous component of east–west shortening. In the Queyfirth Group, the structures are arranged in geometrically and kinematically distinct fault-bounded domains that are interpreted to result from two superimposed tectonic events, the youngest of which displays evidence for bulk dextral transpressional strain partitioning into end-member wrench and contractional strain domains. During dextral transpressional deformation, strain was focused into pelite horizons and favourably aligned pre-existing structures, leaving relicts of older deformation in more competent lithologies. This study highlights the importance of pre-existing structures and lithological heterogeneity during reactivation and suggests the development of a regional transpressional tectonic environment during the Late Carboniferous on the Shetland Platform.

Oblique tectonic interactions are an inevitable consequence of the motion of lithospheric plates on the surface of a sphere (Dewey *et al.* 1998). Despite widespread recognition in ancient and modern settings, many aspects of the evolution of transpressional and transtensional deformation zones remain poorly understood. Transpression is the state of strain that results when convergent displacement is applied obliquely to the boundaries of a deformation zone, whereas transtension is the state of strain that results when divergent displacement is applied (Harland 1971; Dewey *et al.* 1998). Sanderson and Marchini (1984) proposed a simple 3D strain model where a vertical shear zone undergoes thickening (transpression) or thinning (transtension) in response to zone-normal compression or extension, respectively, in addition to significant strike-slip displacements. Numerous additional modifications to this basic model have been proposed (e.g. Tikoff and Fossen 1993; Tikoff and Teyssier 1994; Teyssier *et al.* 1995; Fossen and Tikoff 1997, 1998; Jones *et al.* 1997; Jones and Holdsworth 1998; Holdsworth *et al.* 2002). These include the incorporation of an inclined deformation zone (Jones *et al.* 2004), which leads to transpressional strains with triclinic symmetry (Jones *et al.* 2005), and consideration of the effects of strain partitioning into domains of monoclinic wrench- and contraction-dominated deformation (Tavarnelli 1998; Teyssier and Tikoff 1998).

The documentation of field-based examples of oblique deformation in the upper crust has led to significant improvements in our understanding of transpression and transtension zones (e.g. Tavarnelli *et al.* 2004; Clegg and Holdsworth 2005; Ellero *et al.* 2015). However, few kinematic studies have taken place on transpressional structures that were superimposed on pre-existing folds and associated fabrics. We used field and microstructural observations obtained from a poorly studied part of the Walls Boundary Fault (WBF) in Shetland, Scotland, to explore how

partitioned dextral transpression overprints structures formed during an earlier regional tectonic event.

Geological setting of Shetland and the WBF

The islands of Shetland lie in the centre of the Shetland Platform (Fig. 1a, b), a Mesozoic to present day basement high located NNE of the Scottish mainland. The Shetland Platform is transected by a series of transcurrent faults, the most significant of which is the north–south-striking WBF (Flinn 1977, 1992; Watts *et al.* 2007). The WBF is widely viewed as being the northwards continuation of the Great Glen Fault (GGF) of mainland Scotland (McGeary 1989; Flinn 1992), a major lithospheric strike-slip fault active during the sinistrally transpressional collision of Laurentia and Baltica during the Caledonian orogeny and subsequent transtensional collapse during the Devonian (Dewey and Strachan 2003; Watts *et al.* 2007). The GGF, WBF and related structures were reactivated a number of times during the late Paleozoic, Mesozoic and Cenozoic (Rogers *et al.* 1989; Stewart *et al.* 1999; Watts *et al.* 2007; Le Breton *et al.* 2013; Kemp *et al.* 2019).

Shetland Platform

On Mainland Shetland, the WBF separates two regions of Precambrian–Paleozoic rocks with distinctive geologies that have been correlated with equivalent regions in mainland Scotland (Fig. 1a, b). To the west of the WBF, the Neoarchean Uyea Gneiss Complex has been correlated with the Lewisian Gneiss Complex of the Hebridean Terrane of mainland Scotland (Pringle 1970; Flinn *et al.* 1979; Flinn 1988; however, see also Holdsworth *et al.* 2019; Kinny *et al.* 2019). Structurally overlying the Neoarchean Uyea
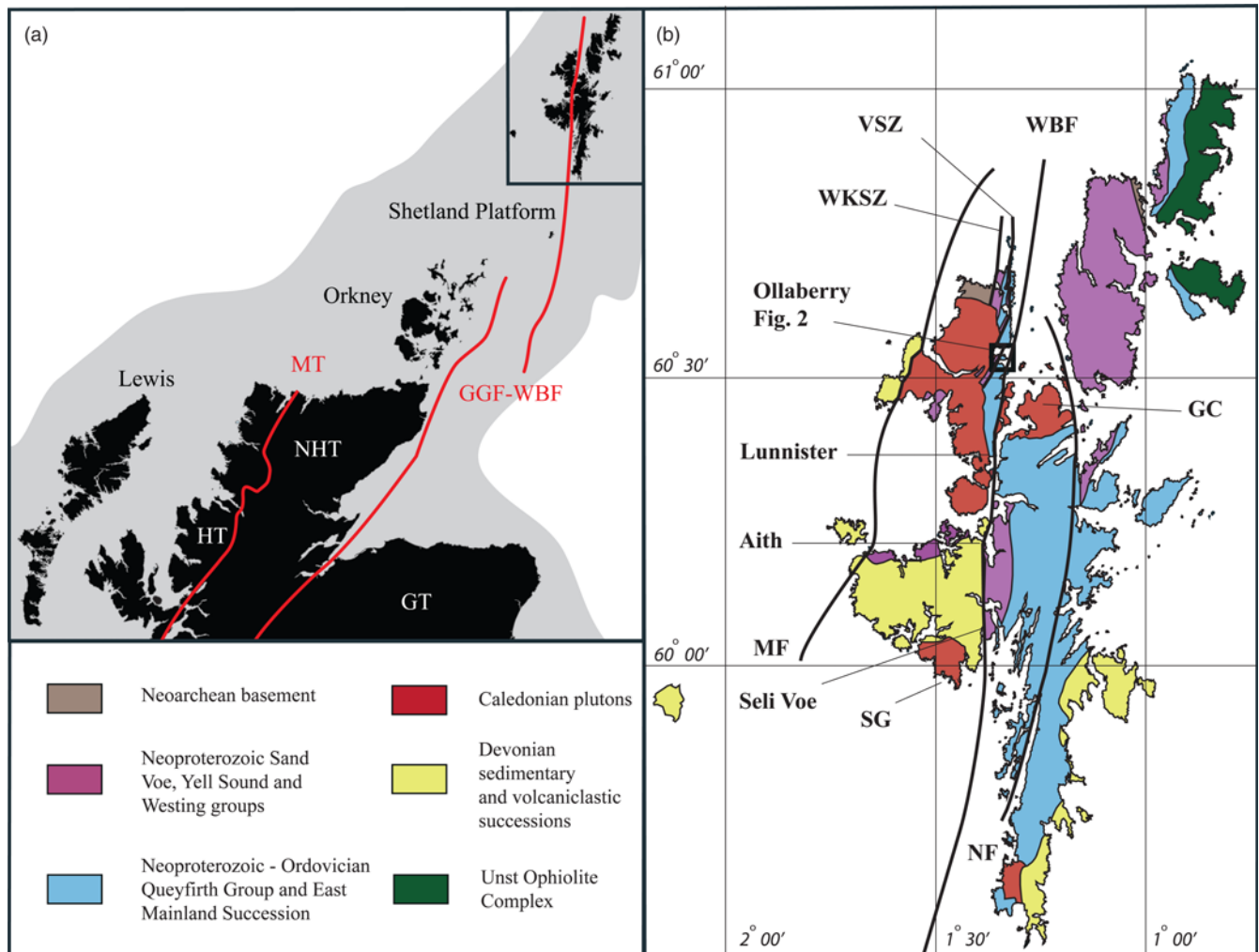
Fig. 1. Location of study area. (**a**) General sketch of NW Scotland, Orkney and Shetland showing the position of the Great Glen–Walls Boundary faults (**b**) Regional map of Shetland showing the main tectonostratigraphic units and tract-bounding faults. GC, Graven Complex; GGF, Great Glen Fault; GT, Grampian Terrane; HT, Hebridean Terrane; MF, Melby Fault; MT, Moine Thrust; NF, Nesting Fault; NHT, Northern Highland Terrane; SG, Sandsting Granite; VSZ, Virdibreck Shear Zone; WKSZ, Wester Keolka Shear Zone; WBF, Walls Boundary Fault.

Gneiss Complex is the metasedimentary Sand Voe Group, which has been correlated with the early Neoproterozoic Moine Supergroup of the Northern Highlands Terrane (Flinn 1988). Interleaved horizons of hornblende-bearing gneiss (the Eastern Gneisses of Pringle 1970) are thought to represent infolds or thrust slices of Archean basement (Flinn 1988). The Wester Keolka Shear Zone, which separates the Uyea Gneiss Complex and the Sand Voe Group, has been correlated with the Moine Thrust, the westernmost limit of Caledonian deformation in mainland Scotland (Andrews 1985; Flinn 1992; Flinn *et al.* 1979; McBride and England 1994; however, see also Walker *et al.* 2016). The Queyfirth Group metasedimentary and metavolcanic rocks structurally overlie the Sand Voe Group and are separated from them by the Virdibreck Shear Zone. The Queyfirth Group has been correlated with the Neoproterozoic–Cambrian Dalradian Supergroup, which underlies much of the Grampian Terrane in mainland Scotland (Flinn 1988).

East of the WBF, the metasedimentary Yell Sound and Westing groups have been correlated with the Moine Supergroup of mainland Scotland (Flinn 1988; Cutts *et al.* 2009, 2011). Succeeding the Yell Sound Group eastwards is the late Neoproterozoic–Cambrian East Mainland Succession, which may correlate with parts of the Dalradian Supergroup (Flinn 1988; Prave *et al.* 2009; Strachan *et al.* 2013). A range of mainly granitic plutons was intruded either side of the WBF between the Late Ordovician (*c.* 465 Ma) and the Late Devonian (*c.* 360 Ma) (Lancaster *et al.* 2017).

The earliest phase of Caledonian deformation on Shetland is represented by the obduction of the Unst Ophiolite Complex. U–Pb zircon dating of the Unst Ophiolite Complex suggests a protolith age of 492 Ma (Spray and Dunning 1991) and that it was obducted during the Grampian orogenic event at 484 Ma (Spray 1988; Flinn 1999, 2001; Crowley and Strachan 2015). Grampian deformation is thought to have resulted from the accretion of a magmatic arc to the Laurentian margin in the Early Ordovician (Ryan and Dewey 1991). Rb–Sr dating of white mica indicates that a north–south-striking regional steep belt had formed in the Yell Sound Group by 480–470 Ma, with localized zones of amphibolite facies metamorphism at *c.* 450 Ma (Walker *et al.* 2016). Grampian ages for the dominant fabric in the Yell Sound Group suggest that the dominant regional ductile fabrics appear to have formed during the Ordovician and that Shetland must have occupied a relatively high structural position during the final Baltica–Laurentia collision in the Scandian (Walker *et al.* 2016).

Onshore Shetland, the Precambrian–Caledonian basement rocks are unconformably overlain by Middle Devonian sedimentary and volcanic rocks, considered to be part of the Orcadian–West Orkney basin system, which extends northwards from NE Scotland to East Greenland (Mykura 1976). Devonian sedimentation is thought to be partly controlled by regional sinistral strike-slip displacement centred on the WBF (Seranne 1992; Watts *et al.* 2007; Wilson *et al.* 2010). Some workers have interpreted folding and faulting of

the Devonian basins to have resulted from Late Carboniferous–Permian brittle–ductile dextral movements along the Walls Boundary, Nesting and possibly Melby faults (e.g. Coward *et al.* 1989; Seranne 1992), whereas others consider the dextral movements to be of Mesozoic age (Flinn 1977, 1992).

Offshore, the Shetland Platform metamorphic basement is overlain by a series of Permo-Triassic extensional basins that are bounded by north–south-trending faults (Duindam and van Hoorn 1987; Ritchie *et al.* 2013). During the Late Jurassic, a major rifting episode uplifted the Shetland Platform and led to widespread erosion (e.g. Richards 1990). Thick sequences of post-rift Cretaceous and Tertiary sedimentary rocks are largely absent, possibly due to further regional uplift and erosion of the Shetland Platform during early Tertiary magmatic underplating of the NW Scottish lithosphere (e.g. Jones *et al.* 2002).

WBF

The WBF is the most geologically significant structural discontinuity transecting Shetland (Flinn 1977, 1992). Seismic surveys of the adjacent continental shelf reveal a lithosphere-scale structure that offsets the Moho and juxtaposes crusts of different thicknesses (McGeary 1989). Onshore, the fault is primarily defined by a zone up to 2 km wide composed of braided, subvertical faults associated with broad zones of cataclasites, phyllosilicate-rich fault gouge and local pseudotachylytes, which formed during dextral strike-slip movements (Watts *et al.* 2007). Importantly, at Lunnister (Fig. 1a), Sali Voe and Aith, fragments of blastomylonitic and mylonitic fault rocks are preserved that indicate an earlier phase of sinistral strike-slip movement (Watts *et al.* 2007). These mylonites are derived from, and interleaved with, banded orthogneisses of similar protolith composition to either the Uyea Gneiss Complex or the Eastern Gneisses (Mykura and Pheminster 1976; Watts *et al.* 2007). Because the igneous Graven Complex (Fig. 2) only preserves evidence of dextral deformation, Watts *et al.* (2007) suggested that older sinistral movement along the WBF initiated prior to its intrusion. Recent U–Pb zircon ages for the Graven Complex suggest emplacement at *c.* 440 Ma (Lancaster *et al.* 2017), which would imply that the fault initiated and sinistral movement commenced no later than the Early Silurian.
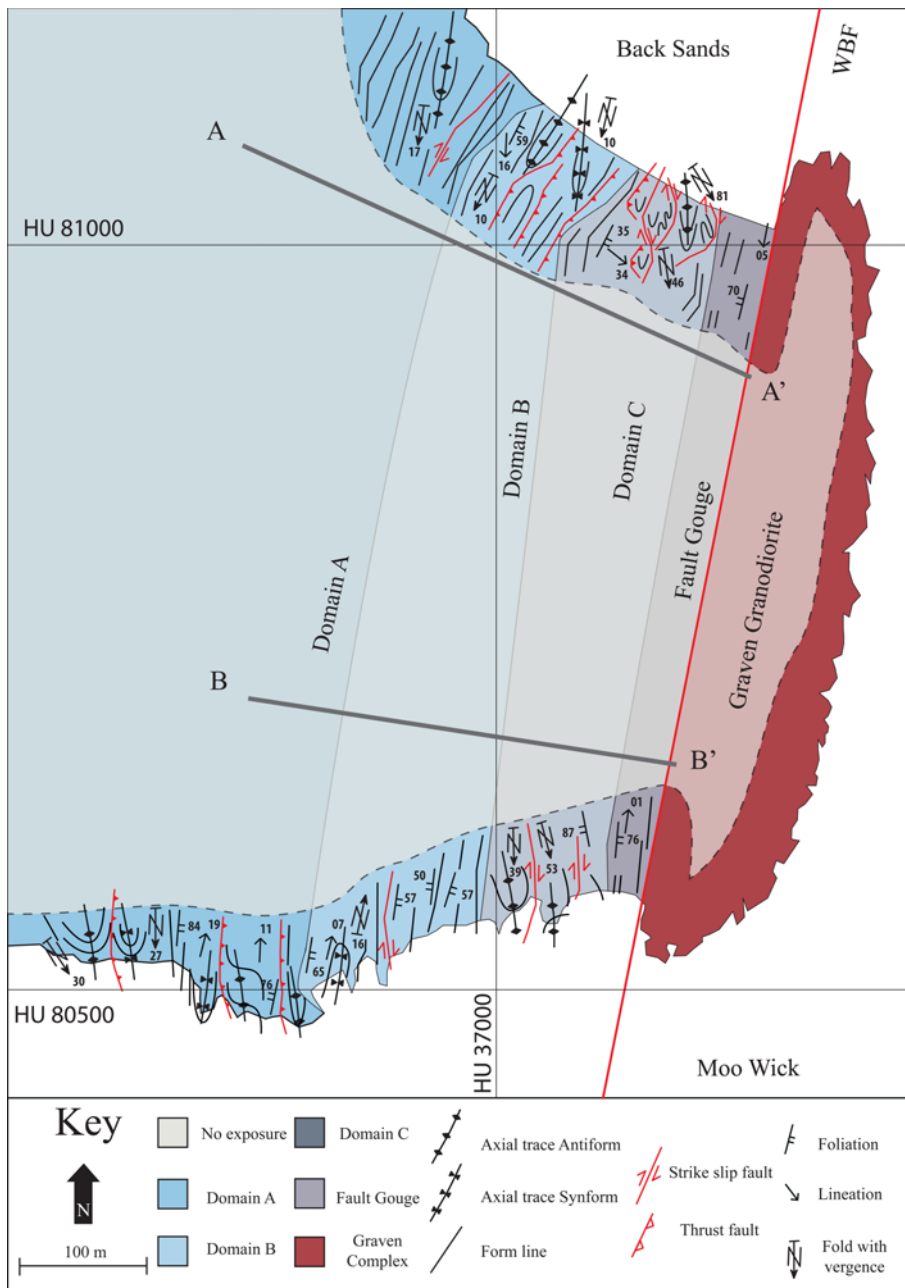
Fig. 2. Structural map of Ollaberry (see Fig. 1b for location). Domains A–C and cross-sections A–A′ and B–B′ are indicated. WBF, Walls Boundary Fault.

Xenoliths of mylonites within the Sandsting Granite (Fig. 1a) are thought to be similar to those at Lunnister (Watts *et al.* 2007). Cross-cutting the mylonite xenoliths and the surrounding granite are brittle cataclasites associated with dextral shearing along the WBF. U–Pb zircon dating of the Sandsting Granite at *c.* 370 Ma provides a lower limit on the initiation of dextral movement on the WBF (Lancaster *et al.* 2017). Interpreting the submarine topography, Flinn (1961) linked the WBF to the GGF, although McBride (1994) used seismic reflection to map a 35 km stepover between the two faults. The magnitude of the early sinistral offset on the WBF is uncertain, although Flinn (1992) suggested at least *c.* 100 km based on the absence of a clear linkage between the pre-Devonian geology either side of the fault. Various workers have proposed Late Carboniferous dextral displacements of up to 95 km on the WBF, based on onshore and offshore correlations and palaeogeographical reconstructions of older Devonian basins and granites (Mykura and Pheminster 1976; Flinn 1977; Rogers *et al.* 1989), although no definitive displacement has been determined (Watts *et al.* 2007).

Watts *et al.* (2007) defined the type locality for the WBF to be at Lunnister, where the best exposed and most complete set of fault rocks is preserved. They further described additional key localities that better preserve other aspects of the fault history. Nevertheless, the sector of the fault at Ollaberry (Fig. 1a) preserves some of the best exposures of the damage zone and remains undocumented in any detail in the published literature. We describe here the geological structures associated with the WBF at Ollaberry, propose a geometric and kinematic model for their development and highlight the key processes that control strain partitioning during transpressional deformation and reactivation. We then summarize the Late Carboniferous deformation in Shetland and mainland Scotland and discuss the implications of our observations for the larger tectonic framework.

Geology of the Ollaberry peninsula

Ollaberry preserves the northernmost exposures of the WBF in Shetland. The Back Sands and Moo Wick beaches on the northern

and southern coastlines of the peninsula, respectively, preserve an almost complete section through the WBF damage zone and fault core (Fig. 2). Two main rock units are exposed: the Queyfirth Group to the west and part of the Graven Complex to the east, which is here represented by a granodiorite (Fig. 2).

Queyfirth Group

The Queyfirth Group forms the eastern coastline of much of the NW Mainland and is composed of quartzites, pelites, limestones and metamorphosed basaltic tuffs (Fig. 1b; Pringle 1970). As a result of its faulted nature, no formal stratigraphic succession has been determined.

At Ollaberry, the Queyfirth Group consists of a generally ESE-dipping sequence of interbanded pelites and impure flaggy quartzites. Layers of quartzite 20–70 cm thick are massive to finely laminated and consist of quartz, orthoclase, plagioclase, minor chlorite and calcite. Pelites consist of muscovite and quartz with minor chlorite, magnetite and plagioclase. Sparse garnet porphyroblasts with inclusion trails of quartz and magnetite are variably retrogressed to chlorite and plagioclase (HU 436991 81106). Locally (HU 36960, 81138 and 36750, 80524), intrusive aphanitic diorites up to 2 m thick of uncertain age in places exhibit concordant and sheared contacts with lithological layering (Fig. 3).

Graven Complex

Regionally, the Graven Complex consists of two superimposed acid to intermediate composition vein complexes, with commonly preserved xenoliths of psammite belonging to the Yell Sound Group. The oldest intrusive phase is represented by veins, pods and dykes of granite and pegmatite, with slightly younger lamprophyre and porphyritic dykes. The youngest phase consists of a network of intrusive sheets of diorite, monzonite, granodiorite and granite with enclaves of hornblendite (Mykura 1976).

At Ollaberry, the granodiorite that forms the Graven Complex is composed of roughly equigranular coarse- to medium-grained
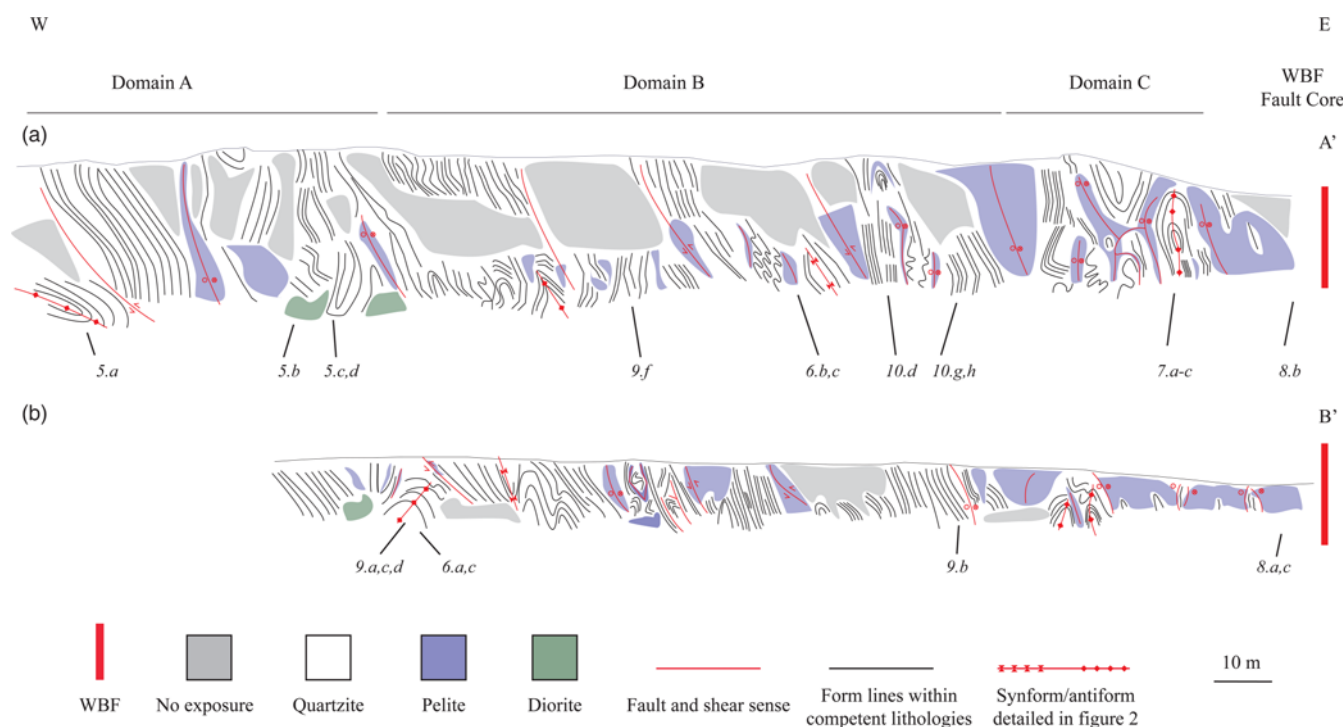
Fig. 3. Schematic cross-sections of (**a**) Back Sands and (**b**) Moo Wick, with locations of Figures 5–10. Note the increase in pelite closer to the Walls Boundary Fault. WBF, Walls Boundary Fault.

quartz, K-feldspar, epidote, chlorite and minor biotite. No magmatic or ductile fabric is present and enclaves of mafic material up to 10 cm across occur locally. Late-stage pegmatitic veins up to 3 cm thick cross-cut the main intrusion.

Field observations at Back Sands and Moo Wick

Detailed mapping of the Back Sands and Moo Wick sections reveals a heterogeneous deformation pattern of NNE–SSW-trending fault-bounded domains (here termed A–C) in the Queyfirth Group (Figs 2–4). In Domains A–C, kinematically and geometrically different structures, some inferred to be of broadly the same age, are recognized on millimetre to decimetre scales. Figure 2 shows a detailed geological map surveyed by a mixture of cairn mapping and drone aerial photography. Figure 3 shows composite east–west cross-sections from Moo Wick and Back Sands, constructed from field observations and drone photogrammetry. Figure 4 provides stereonets that record the orientations of the main structures observed in each domain.

The domains are described from west to east moving progressively closer to the WBF core. Based on field relationships, one poorly preserved and two widely recognized deformation phases are observed, termed here 'Proto', 'Early' and 'Late'. This nomenclature is used in preference to the more traditional D numbers in recognition that individual sets of structures may be of local rather than regional significance. Note that Domain A corresponds to the western limit of demonstrably WBF-related deformation in the Ollaberry area.
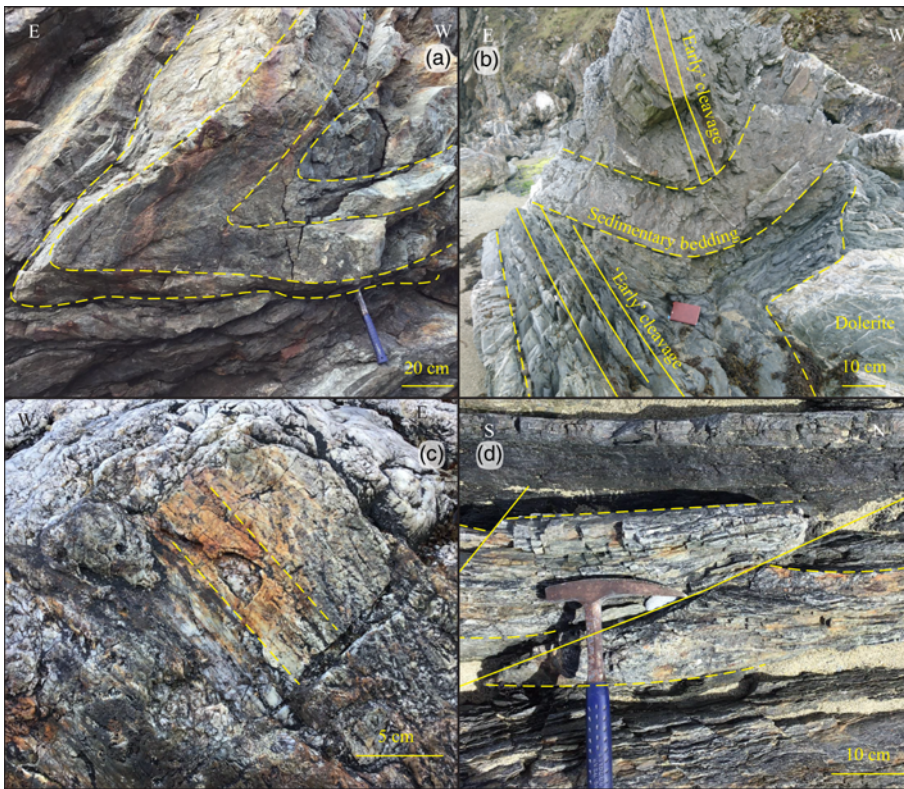
Domain A

Domain A represents the westernmost zone of WBF-related deformation between 300 and 175 m west of the WBF core. This domain is dominated by 'Early' ductile structures with localized zones of 'Late' brittle–ductile deformation. Overall, Domain A forms an ESE-dipping homocline indicated by a well-defined maximum of poles to foliation (Figs 2, 3 and 4ai). Elongated quartz rods and mica grains form a sub-horizontal to moderately plunging, NNE-trending stretching mineral lineation.

Mesoscale, tight to isoclinal, curvilinear 'Early' folds plunge shallowly to moderately north or south, with upright to inclined axial planes verging west (Figs 4aii and 5a). A cleavage is well developed roughly parallel to the fold axial planes (Figs 4aiii and 5b). Cleavage–foliation intersection lineations are sub-parallel to 'Early' fold hinges (Fig. 4aiv). Within the pelite horizons, minor 'Late' structures include tight millimetre- to centimetre-scale microfolds and kink bands that plunge vertically to steeply north or south, with axial planes striking NW–SE and a Z-verging dextral shear sense. Overall, however, refolding of the 'Early' cleavage by 'Late' deformation structures is minor in Domain A.

Within Domain A, NNE–SSW faults are mostly confined to pelite horizons and show predominantly steeply dipping, anastomosing geometries. S-C fabrics and slickenlines suggest two main fault sets that are identified with reverse and dextral strike-slip shear senses, respectively (Figs 4avi, 5c, d). Both are associated with the development of blue, incohesive, foliated clay fault gouges up to 5 cm thick; breccia development is limited.
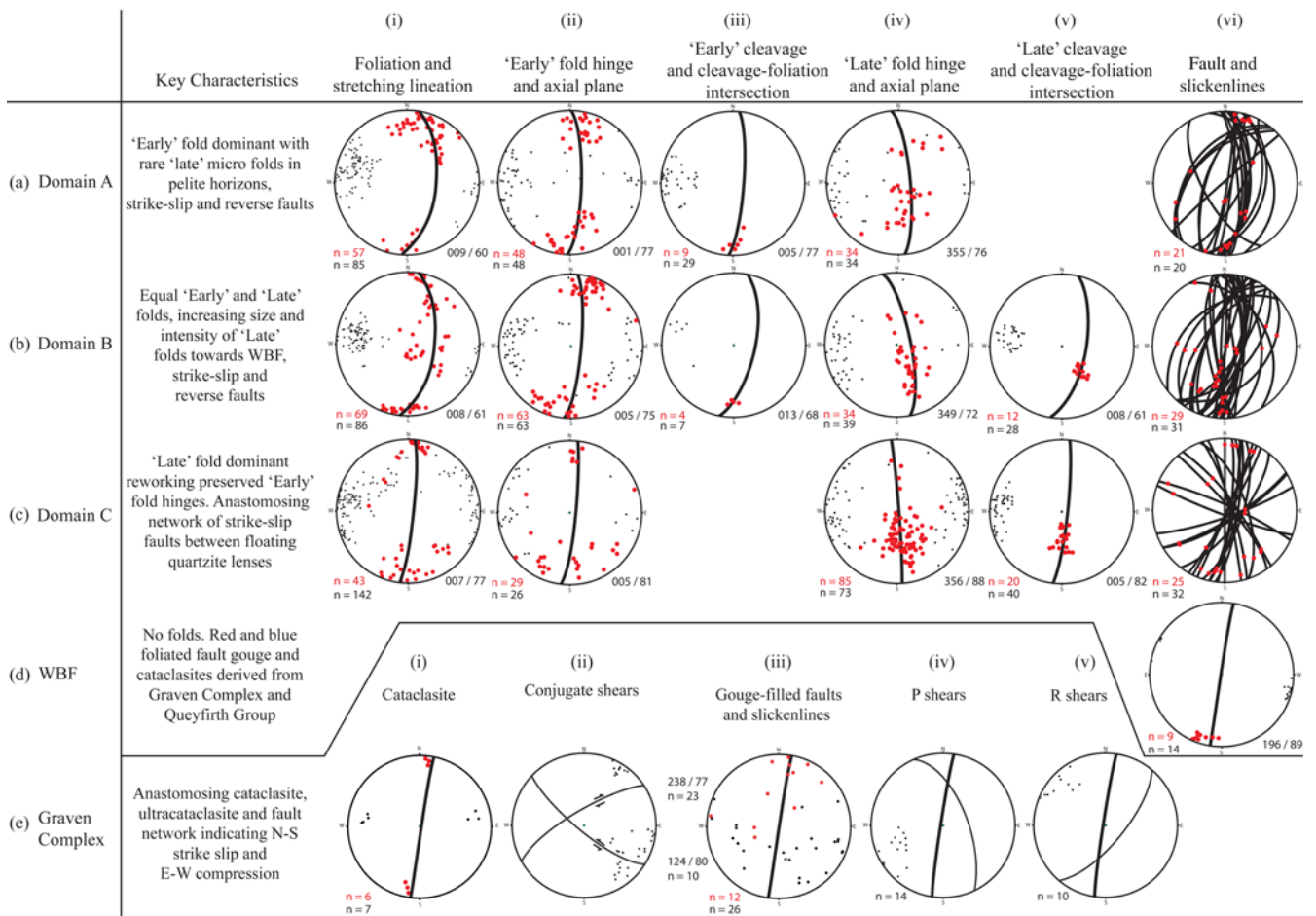
Fig. 4. Orientation data from (**a–c**) Domains A–C, (**d**) fault core and (**e**) Graven Complex. Lower hemisphere, equal-area projections. For columns (i–v), planar measurements are indicated as black pole-to-plane dots and have a mean plane drawn and noted. Linear measurements are represented as red dots. The number of measurements for structures are given by '*n*'. For column (vi), faults are graphically represented as planes. WBF, Walls Boundary Fault.

Fig. 5. Summary of the features observed in Domain A at Ollaberry. (**a**) A tight 'Early' fold with an inclined axial plane and moderately plunging hinge (HU 36960, 81138). (**b**) 'Early' west-vergent fold in Domain B of Moo Wick (HU 36708, 81099). (**c**) Fault plane showing top-to-the-west slickenlines associated with contractional 'Late' deformation (HU 36985, 81100). (**d**) Dextrally offset quartzite layer (HU 36990, 81092).

Domain B

Located between 175 and 60 m from the WBF plane, Domain B is characterized by more common 'Late' structures that variably overprint 'Early' west-verging folds. Domain B contains more prominent quartzite horizons than Domain A and forms an overall homoclinal sequence of steeply east-dipping metasediments. Mineral stretching lineations form a variable range of north–south shallowly plunging to steeply east-plunging trends, indicating a variety of slip vectors along a north–south girdle (Fig. 4bi).

Quartzite horizons display mesoscale upright to inclined, tight to isoclinal 'Early' folds (Fig. 6a). The limbs of 'Early' folds are often boudinaged, indicating a substantial component of ductile shearing following fold formation. 'Early' fold hinges are curvilinear and variably plunge shallowly NNE or SSW (Fig. 4bii). The folds are west-vergent and the axial planes strike NNE–SSW (Figs 3 and 6a). Fold pairs are commonly discontinuous, with some hinges being truncated by faults and phyllosilicate-rich gouge, indicating later reworking. A strong axial planar cleavage and intersection lineation is developed in pelites (Fig. 4biii).

'Late' structures include centimetre-scale kink bands that show Z-shaped dextral vergence in map view. Associated with the kink bands is a weak crenulation cleavage and microscale to mesoscale folds that are well developed within pelite and interbedded pelite–quartzite horizons (Fig. 6b). Hinge orientations are highly curvilinear, plunging shallowly to steeply along a NW–SE girdle (Fig. 4biv), and become increasingly variable towards the WBF. The axial planes and axial planar cleavage strike NNE/NNW–SSW/SSE (Fig. 4biv, v).

An early 'Proto' cleavage, defined by the alignment of micas and quartz, is preserved locally in 'Early' fold hinges. This foliation is oblique to the sedimentary bedding, defined by a change in lithology, and both are folded by 'Early' fold hinges and cross-cut by 'Early' cleavages (Fig. 6c). Adjacent outcrops of 'Proto' cleavage display opposite angular relationships between the cleavage and bedding. In all other localities at Ollaberry, 'Proto' cleavage and sedimentary bedding are sub-parallel and indistinguishable. This geometry suggests that a 'Proto' phase of folding, with associated axial planar cleavage, may have formed prior to 'Early' deformation and is either poorly preserved elsewhere and/or is indistinguishable from 'Early' fold structures.

Reverse dip-slip and dextral strike-slip faults are widely developed in Domain B (Figs 2, 3 and 4bvi). Faults are preferentially developed in the pelite horizons and are defined by 5–10 cm thick blue foliated gouges. Dip-slip faults mostly dip east and display top-to-the-west shear bands and stepping slickenlines. Reverse-slip slickenlines typically plunge moderately to steeply east downdip or slightly oblique to the associated fault planes. Strike-slip faults, identified by dextrally sheared bands and offset markers, are subvertically NE–SW-trending with horizontal slickenlines (Fig. 6d).

Domain C

Located between *c.* 60 m and the fault core, Domain C is composed of phyllosilicate-rich sheared material derived from pelite enveloping highly deformed, 10 m-scale quartzite lenses. Foliation developed in quartzite blocks lies on an east–west girdle folded around a β-axis that moderately dips to the south. Mineral stretching lineations plunge shallowly north–south (Fig. 4ci).

Within the quartzite horizons, discontinuous hinges of mesoscale, tight to isoclinal 'Early' folds are only locally preserved. Fold limbs are sheared out or faulted. Fold hinges plunge shallowly to moderately north or south and the axial planes are mostly upright to inclined (Fig. 4cii) and indicate a general westwards vergence (Fig. 3). These folds are reworked by open to tight, highly curvilinear 'Late' folds with an overall Z dextral vergence (Fig. 7). Centimetre-scale kink bands are developed in the sheared pelites between quartzite lenses and display parallel hinge and axial plane geometries to the 'Late' folds. The 'Late' folds display variable shallowly south–SE to subvertical plunges spread out along a girdle parallel to their mean axial plane (Fig. 4civ). Axial planes are steeply ENE-inclined to vertical and strike NNW–SSE. Refolding of 'Early' folds during 'Later' deformation results predominantly in 'Type-2' and, in places, 'Type-3' interference patterns (*sensu* Ramsay 1967) (Fig. 7c). The 'Late' cleavage is well developed in

Fig. 6. Summary of the features found in Domain B at Ollaberry. (**a**) 'Early' west-verging fold hinge (HU 36872, 80517). (**b**) Dextrally verging 'Late' folds in pelite (HU37037, 81044). (**c**) 'Proto' cleavage preserved in an 'Early' fold hinge. 'Proto' fabric is oblique to original sedimentary bedding in multiple outcrops, indicating a poorly preserved 'Proto' deformation phase (HU 37021, 81080). (**d**) Dextrally offset quartzite layer (HU 37027, 81060).

the pelite horizons and forms a concentrated pole to cleavage population (Fig. 4cv). Here, the cleavage dips steeply east, with crenulation intersection lineations plunging moderately to steeply on a north–south great circle.

Subvertical fault planes are infilled by 10–15 cm thick horizons of highly sheared gouge containing brecciated quartz clasts. Fault planes are concentrated along pelite horizons and border 'floating', highly deformed quartzite lenses in an anastomosing array of interconnected fault planes (Fig. 7a, b). Faults strike typically NNE–SSW, sub-parallel to the WBF plane, and display sub-horizontal slickenlines (Fig. 4cvi). Within the sheared fault gouge horizons, a strong vertical north–south-striking fabric with sub-horizontal
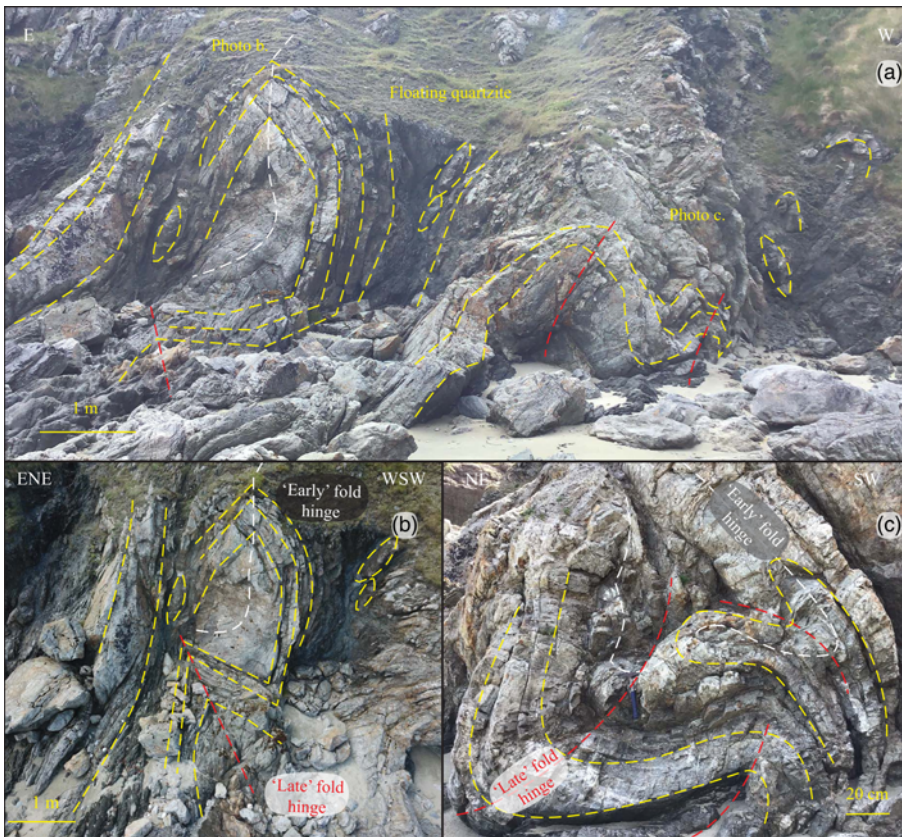
Fig. 7. Examples of interference patterns between 'Early' and 'Late' folds in Domain C at Back Sands (HU 37110, 81000). (**a**) Highly deformed quartzite lenses 'float' between phyllosilicate-rich sheared pelites. Quartzite lenses show decimetre-scale, upright, west-vergent 'Early' fold hinges. (**b**) Close-up of part (a). Limbs of favourably aligned 'Early' folds are sheared and replaced with phyllosilicate-rich fault gouge. (**c**) Close-up of part (a). Type 2 fold interference pattern between 'Early' and 'Late' folds. Yellow lines, foliation trace; white lines, 'Early' fold trace; red lines, 'Late' fold trace.
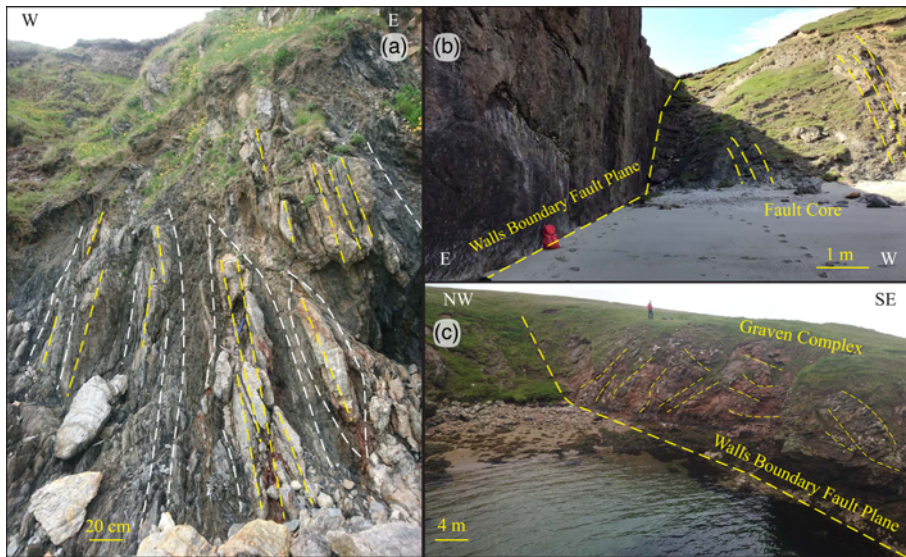
Fig. 8. Summary of the structures found in the fault core, Walls Boundary Fault plane and Graven Complex. (**a**) Highly sheared floating quartzite lenses in a phyllosilicate-rich matrix derived from pelites in the fault core (HU37061, 80582). (**b**) Clearly exposed Walls Boundary Fault plane marking the contact between the fault core and the Graven Complex (HU 37157, 81011). (**c**) Walls Boundary Fault plane and Graven Complex. Graven Complex shows criss-crossing cataclasites (HU37073, 80563).

lineations is associated with dextral S-C′ fabrics and centimetre-scale kink bands.

Fault core, WBF and Graven Complex

The WBF core is a *c.* 10 m thick, poorly exposed area between the WBF fault plane and the Queyfirth Group. It is composed of cataclasites derived from both the Queyfirth Group and the Graven Complex. Blue and red clay fault gouges *c.* 1 m thick are interleaved with the cataclasite and display a subvertical, fault-parallel fabric defined by colour banding and alignments of phyllosilicate minerals (Fig. 8a, b). Clasts of cataclasite commonly occur within the red gouge, suggesting that the latter is younger. The exposed WBF plane strikes vertically NNE–SSW with sub-horizontal slickenlines (Fig. 4dvi), indicating strike-slip movement; however, no shear sense can be determined.

East of the WBF, 100 m of granodiorite forms the eastern end of the Ollaberry Peninsula (Fig. 2). The Graven Complex here is cut by numerous mutually cross-cutting structures. Cataclasite to ultracataclasite seams several centimetres thick form a series of anastomosing north–south-striking faults orientated sub-parallel to the WBF core (Figs 4ei and 8c) that are infilled with dextrally stepping quartz fibres. Cataclasites and ultracataclasites often envelope fractured granitic clasts on a micro- to mesoscale. The clasts are irregularly orientated north–south.

Seams of fractured granodiorite and ultracataclasite are mutually cross-cut by conjugate sinistral and dextral faults, which typically show offsets of up to several centimetres. These fractures trend subvertically SW–NE and NW–SE, respectively (Fig. 4eii). The cataclasites, ultracataclasites and conjugate shear fractures mutually cross-cut earlier gouge-filled faults locally (Fig. 4eiii). These faults contain red and blue clay gouge and bound slices of relatively undeformed pegmatitic granite. Two subsets of subvertical faults are orientated NNW–SSE anticlockwise and NNE–SSW clockwise of the WBF, respectively. Both contain slickenlines and offset markers indicating dextral movements. These are interpreted, respectively, as P and R shears in an overall dextral shear regime (Fig. 4eiv, v).

Microstructures

Thin sections were taken from quartzite and pelite units to ascertain the pressure–temperature conditions, deformation mechanisms and the relationships among the 'Proto', 'Early' and 'Late' deformations. Thin sections could not be obtained from the fault gouges due to their fragility. Sections were cut perpendicular to the foliation and parallel to lineation or, where folds were examined, normal to the fold hinges. The recrystallization of quartz via either bulging, sub-grain rotation or grain boundary migration is primarily dependent on temperature and strain rate and is used here to estimate the deformation conditions (e.g. Hirth and Tullis 1992; Kruhl 1998; Stipp *et al.* 2002). This method is cross-referenced with mineral assemblages and feldspar deformation microstructures (Passchier and Trouw 2005).

'Proto' and 'Early' deformation

Quartzite and pelite samples taken from 'Early' fold hinges (Fig. 9a, b, see also Fig. 6c) show a strong foliation defined by the alternation of quartz-rich and muscovite-rich layers, interpreted to be relict sedimentary layering. Quartz is recrystallized as medium- to fine-grained (0.1–0.5 mm), equigranular and polygonal grains with a shape-preferred orientation (SPO) and weak lattice-preferred orientation (LPO), indicating a dominance of sub-grain rotation recrystallization processes (Fig. 9c, d). Quartz ribbon aggregates bounded by interstitial muscovite are coarser grained (0.6–0.8 mm) relative to the adjacent polymineralic domains and show grain boundary (Zenner) pinning effects (e.g. Evans *et al.* 2001).

Lying oblique to the layering, an alignment of fine-grained (0.1–0.3 mm) muscovite grains defines a distinctive foliation. This alignment is thought to be related to the earliest 'Proto' deformation because it is demonstrably folded by the closely spaced crenulation cleavage that is axial planar to the 'Early' folds (Fig. 9a). Relict clasts of coarse-grained (0.5–0.8 mm) quartz and feldspar grains with sweeping undulose extinction are observed with an LPO oblique to the foliation (Fig. 9e). Strain shadows infilled with muscovite and recrystalized quartz are observed proximal to the relict clasts. Feldspars show sweeping undulose extinction, no twinning or kinking, and no evidence of dynamic recrystallization. Rare sinistrally sheared garnets that are partly retrogressed to chlorite are present within quartzite-rich horizons (Fig. 9f). Within the garnets, inclusions of plagioclase and quartz are aligned oblique to the 'Early' foliation, demonstrating that the garnets grew prior to 'Early' deformation (Fig. 9f). Our preferred interpretation is that this early inclusion fabric corresponds to the 'Proto' deformation fabric.

Based on the mineral assemblage and preserved deformation microstructures, the 'Early' deformation is estimated to have occurred at mid- to lower greenschist facies (*c.* 400°C) temperatures.
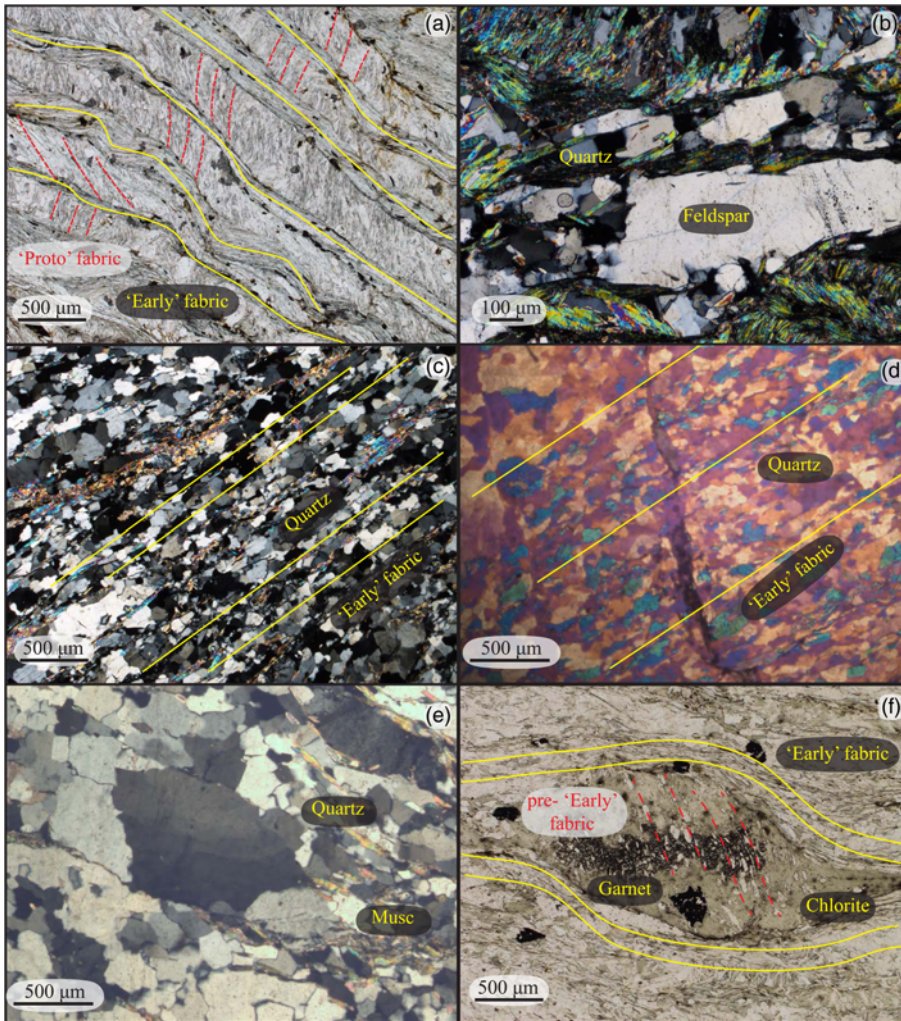
Fig. 9. Photomicrographs taken in plane polarized light (PPL) or crossed polarized light (XPL). (**a**) Reworking of previous fabric in a pelite sample from Domain B, Moo Wick (PPL, HU 36871, 80520). (**b**) Brittle deformed feldspar in quartzite sample, indicating *c*. 400°C temperature for 'Early' deformation, from Domain B, Moo Wick (XPL, HU 36998, 81074). (**c**) Equigranular polygonal quartz in quartzite, from Domain B, Back Sands (XPL, HU 36871, 80520). (**d**) Equigranular polygonal quartz in quartzite showing lattice-preferred orientation, Domain B, Back Sands (XPL, HU 36871, 80520). (**e**) Relict quartz grain showing sweeping undulose extinction and lattice-preferred orientation oblique to the samples, 'Early' fabric, from Domain B (XPL). (**f**) Sinistrally sheared pre-'Early' deformation garnet in quartzite sample, extensively replaced with chlorite, Domain B, Moo Wick (PPL, HU 37067, 81030).

The deformation conditions during the earlier 'Proto' event are uncertain, but probably reached at least garnet grade.

'Late' deformation

Late structures are best observed in pelite samples taken from Domains B and C near to the WBF. Fine-grained (0.1–0.2 mm) muscovite defines a penetrative foliation and shows a strong SPO and LPO (Fig. 10a). Muscovite grains are subhedral, acicular and lozenged-shaped with their cleavage orientated parallel to the SPO, consistent with slip along the 001 plane (ten Grotenhuis *et al.* 2003). No kinking or folding and little undulose extinction is observed in the muscovite grains. In places, the muscovite grains orientated parallel to 'Late' foliation truncate and overgrow 'Early' muscovite (Fig. 10b). Interstitial to the muscovite grains are quartz sub-grains that show polygonal and equigranular textures with a weak to no SPO and LPO (Fig. 10c). The quartz grain size is dependent on the mica content, varying from medium- (0.4 mm) to very fine- (<0.2 mm) grained in high- and low-percentage mica, respectively (Fig. 10c, d). No undulose extinction, kinking or deformation lamellae are observed and the quartz grains are relatively strain-free (Fig. 10c, d). Quartz ribbons, along with interstitial muscovite, are dextrally sheared in S-C fabrics, indicating that they were subject to 'Late' deformation (Fig. 10e). Parallel to muscovite and truncating the quartz and feldspar grains are dark (opaque) seams of hematite and other insoluble material surrounding phenocrysts of rounded quartz and plagioclase grains (Fig. 10f). The presence of dark (opaque) seams indicates dissolution and precipitation in pressure solution (e.g. Rutter 1983). Voluminous amounts of very

fine-grained sericite, chlorite and thick tabular twinned calcite overgrow quartz and muscovite rims, often forming saddle reef structures in 'Late' fold hinges (Fig. 10g). Sericite, chlorite and calcite are interpreted as characteristic 'Late' deformation minerals based on their association with syntectonic 'Late' microstructures.

Quartzites sampled close to the WBF in 'Late' fold hinges are medium to fine grained (0.2–0.4 mm) and surrounded by very fine grained (<0.1 mm) recrystallized quartz sub-grains (Fig. 9d, h). Quartz sub-grains are equigranular and polygonal and display an SPO and LPO and sweeping undulose extinction (Fig. 10h). Collectively, the observations on quartz indicate that it was deformed via sub-grain rotation and was subject to a low-temperature reworking of previously recrystallized material. Minor fine-grained (0.2 mm) muscovite is observed interstitial to quartz. Voluminous calcite and fine-grained muscovite (0.1–0.2 mm) overgrow quartz (Fig. 10d) and are interpreted to have grown syntectonically with the 'Late' deformation. Rare garnets are extensively replaced with chlorite. Collectively, the mineral assemblage, calcite twins and deformation mechanisms are interpreted to indicate lower greenschist–zeolite facies (300–150°C) temperatures for the 'Late' deformation.

Discussion

Relative ages of structures

Given the heterogeneity of the deformational and kinematic patterns at Ollaberry, it is essential to establish the relative age relationships of the various structures observed in the deformation domains. Within Domain B, outcrops of 'Early' fold hinges preserve a 'Proto'
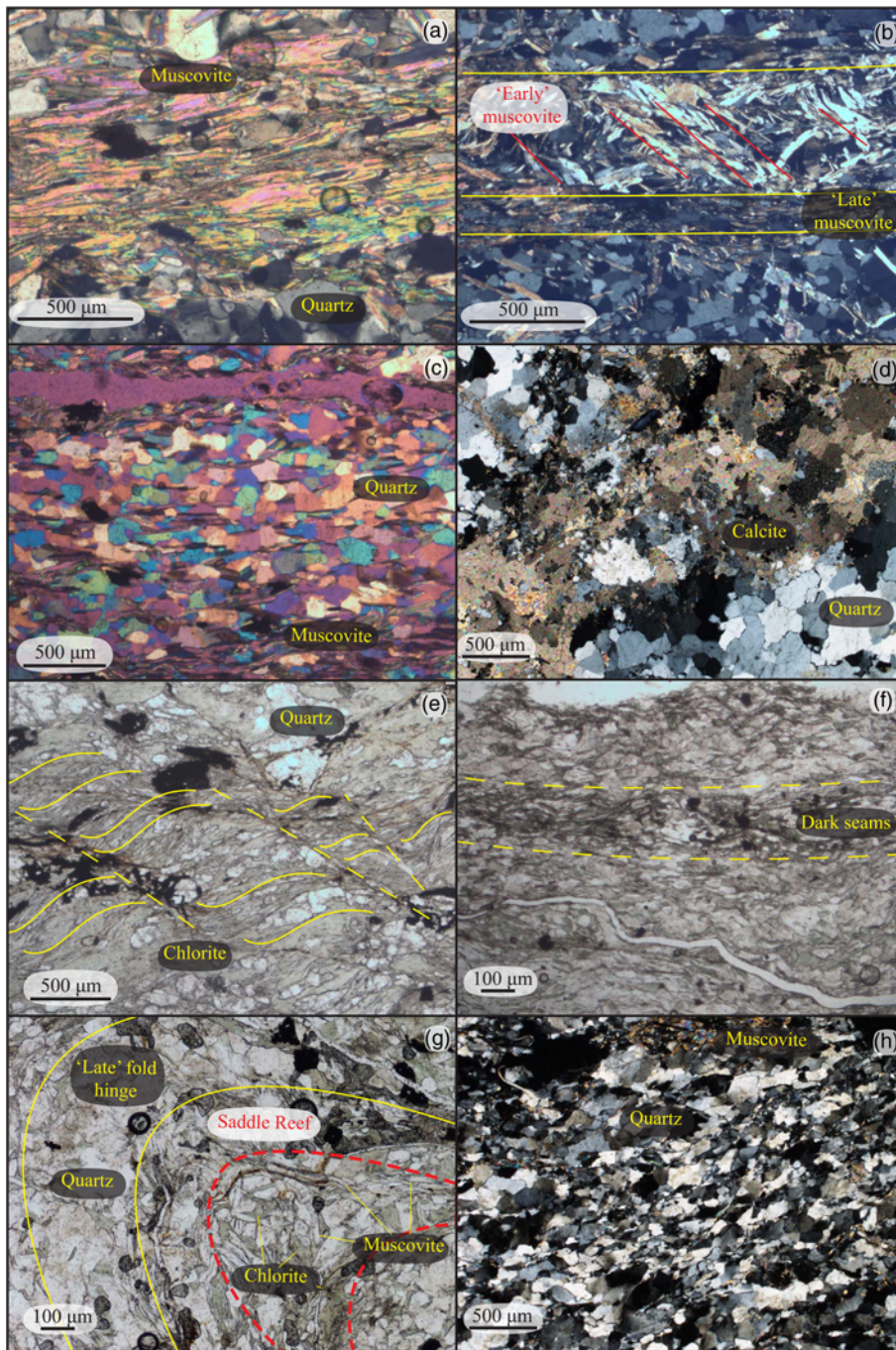
Fig. 10. Photomicrographs taken in plane polarized light (PPL) or crossed polarized light (XPL). (**a**) Muscovite showing strong shape-preferred orientation and lattice-preferred orientation (XPL, Domain B). (**b**) 'Early' muscovite grains truncated and overgrown by 'Late' muscovite in a pelite (XPL, Domain B). (**c**) Quartzite with interstitial muscovite showing moderate shape-preferred orientation and no lattice-preferred orientation (XPL with tint plate inserted, Domain B). (**d**) Quartz overgrown by calcite during 'Late' deformation in quartzite sample, Domain B, Back Sands (XPL, HU 37029, 81053). (**e**) Dextrally sheared S-C′ fabric in pelite. Muscovite has been extensively replaced with chlorite and minor calcite. (PPL, Domain C). (**f**) Dark seams of opaque material in surrounding mica-rich horizon (PPL, Domain B). (**g**) 'Late' fold hinge, defined with yellow form lines, with chlorite and muscovite forming in a 'Late' saddle reef structure, defined with red lines. Pelite sample, Domain C, Back Sands (PPL, HU 37096, 81002). (**h**) Quartz grains overgrown by 'Late' muscovite. Quartz grains display sweeping undulose extinction closer to the Walls Boundary Fault, quartzite sample, Domain C, Back Sands (XPL, HU 37096, 81002).

cleavage oblique to the sedimentary bedding. The 'Proto' cleavage and sedimentary bedding display opposite angular relationships, suggesting that a set of 'Proto' folds were formed before 'Early' deformation, but are not well preserved or always distinguishable from 'Early' and 'Late' deformation structures.

Domains A–C display differing patterns of fold characteristics, geometry and intensity. West-vergent, tight to isoclinal 'Early' folds are, however, observed in all domains and show axial planes parallel to the regional cleavage, suggesting that these structures are contemporaneous. Z-shaped dextral folds that steeply plunge SE are considered 'Late' structures. 'Late' structures become increasingly prevalent, larger scale and curvilinear towards the WBF. The dextral folds overprint west-vergent folds in Domain C and parts of Domain B, confirming the 'Late' and 'Early' relationship, respectively.

Faults in the Queyfirth Group are marked by foliated clay gouges and are concentrated in phyllosilicate-rich pelite units, or along lithological contacts. Slickenlines and shear sense indicators on faults in all domains display a mixture of strike-slip, oblique and top-to-the-west reverse geometries. Based on the lithological similarity between all fault zones and the kinematic similarity of 'Late' folds and faults, these are assumed to have formed broadly contemporaneously. Brittle deformation in the Graven Complex shows a complex cross-cutting relationship between cataclasite– ultracataclasite-conjugate faults-gouges. Fault slickenlines, offset markers and riedal shear orientations suggest that the broad deformation pattern observed is north-south dextral strike-slip and east-west contraction. The geometry of structures in the Graven Complex is kinematically compatible with the 'Late' deformation observed in the Queyfirth Group and suggests that all these structures are contemporaneous.

The fault core shows poorly preserved sub-horizontal slick-enlines in the fault gouge, indicating strike-slip movement. It is unknown whether the strike-slip shearing seen in the core is wholly or partially related to the 'Late' deformation or whether it is related to the younger sinistral strike-slip event of possible Cenozoic age recognized by Watts *et al.* (2007) in some other parts of the WBF.

Kinematic model

A geometric model and synopsis of the structural evolution (Figs 11 and 12) are presented to account for the kinematic observations recorded. We propose that the Queyfirth Group initially developed a 'Proto' cleavage under garnet grade metamorphic conditions, overprinted by mesoscale tight-isoclinal 'Early' folds characterized by westerly verging, shallowly north- or south-plunging fold hinges and east-dipping axial planes formed in an east–west contractional regime. Currently, it is difficult to say with any certainty the age of sinistral shear on the WBF relative to 'Proto' and 'Early' deformation.

During 'Late' deformation, kinematic indicators suggest a combination of contemporaneous top-to-the-west reverse and dextral strike-slip movements on, respectively, steeply inclined faults and dextrally vergent Z-folds. These concurrent kinematics are consistent with top-to-the-west and dextral domainal monoclinic transpressional deformation (Fig. 12c). Domains A and B exhibit a combination of dextral folding within pelite horizons and strike-slip and reverse shear sense along faults, suggesting a kinematic partitioning of the wrench strain into faults and folds, whereas contractional strain was mostly accommodated by faults. Domain C, however, solely displays dextrally sheared folds and faults, suggesting that, closer to the WBF, wrench transpressional strain became dominant with the localization of 'Late' deformation into phyllosilicate-rich pelite units. In the Graven Complex, brittle cataclasites and ultracataclasites display P and R shears, dextrally stepping quartz fibres and conjugate east–west reverse faults. These structures are also thought to be simultaneous with deformation in the Queyfirth Group and indicate a bulk wrench domainal monoclinic strain regime with a minor reverse component (Fig. 12).

Controls on kinematic partitioning

Many studies (e.g. Tavarnelli and Holdsworth 1999; Holdsworth et al. 2002; Tavarnelli et al. 2004; McCaffrey et al. 2005) have demonstrated that transpression can be partitioned into end-member wrench and shortening components across a wide range of scales. Many workers (e.g. Tikoff and Teyssier 1994; Teyssier et al. 1995) have suggested that the kinematic partitioning of strain in transpression zones is primarily controlled by the relative angle of convergence and assume a simple, homogeneous rheology.

Field observations at Ollaberry suggest that wrench shear during the 'Later' deformation event (dextral folding and faulting) was preferentially focused into phyllosilicate-rich pelite horizons. A marked increase in the pre-existing anisotropy in Domain C may then also explain why 'Late' wrench dextral shear displacements were partitioned close to the WBF, whereas equivalent-age deformation in Domains A and B also involved components of top-to-the-west contraction – that is, the observed kinematic partitioning was controlled by the pre-existing lithologies and mechanical anisotropy. However, it must be noted that, on all scales, the degree of partitioning is never 100% – for example, wrench-dominated domains, such as Domain C, always preserve subordinate sets of structures with a component of reverse movement.

Microstructural observations from quartzites show that the quartz grains were primarily deformed via sub-grain rotation, probably during 'Early' deformation. Quartzites close to the WBF are overgrown by a calcite–chlorite mineral assemblage and display a sweeping undulose extinction, indicating lower temperature reworking during 'Late' deformation. In the pelite samples representative of 'Late' deformation, the quartz grains show less indication of low-temperature reworking and appear strain-free. Micas, on the other hand, display strong SPO and LPO alignment and are dextrally sheared, probably via layer-parallel slip and pressure solution from 'Late' deformation. Collectively, the microstructural observations suggest that 'Late' deformation was focused into mechanically weaker muscovite on a microscale, with quartz aggregates behaving as passive markers.
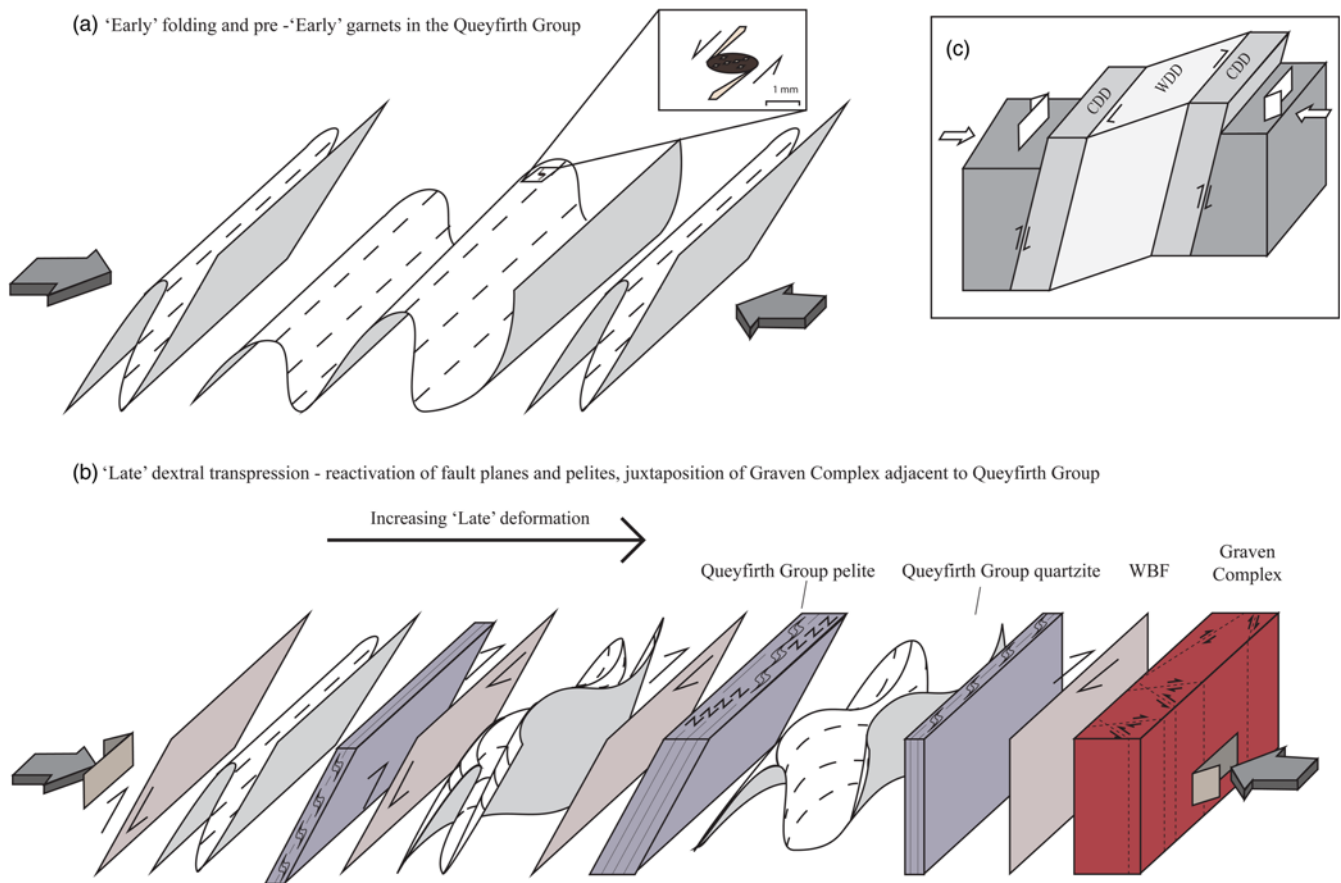
The overall conclusion is that, in addition to far-field controls such as the convergence angle, the structural and kinematic
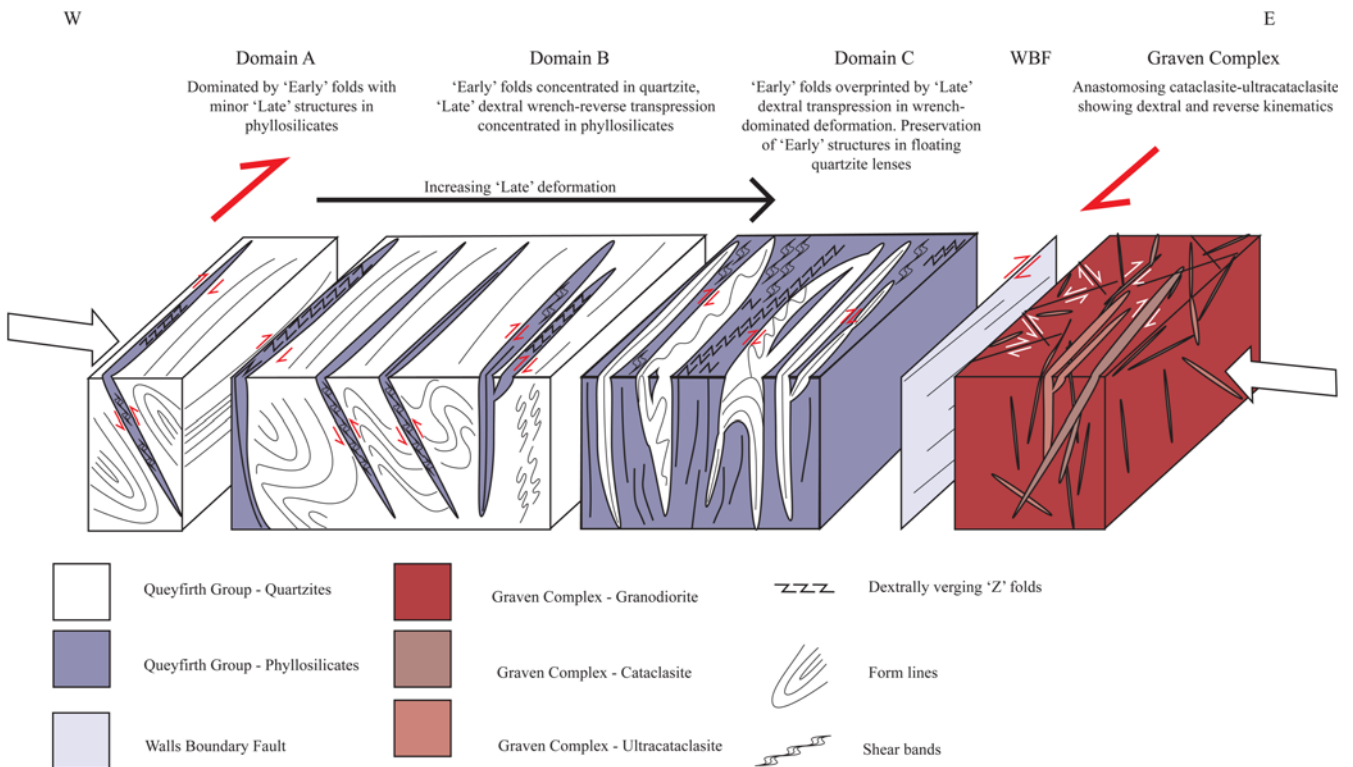
Fig. 11. Block diagram summarizing the structures observed at Ollaberry and the kinematic model proposed for the Walls Boundary Fault.

Fig. 12. (**a**, **b**) Kinematic model for 'Proto', 'Early' and 'Late' deformation at Ollaberry. (**c**) Schematic 3D model in which monoclinic transpressional strain is partitioned into end-member wrench-dominated and contraction-dominated domains. CDD, contraction-dominated domain; WBF, Walls Boundary Fault; WDD, wrench-dominated domain.

evolution of a transpressional deformation zone will also be strongly influenced by pre-existing mechanical and microstructural properties and the layering orientations of the host rock successions.

Tectonic evolution of the WBF

Regional mapping by Pringle (1970) in the Queyfirth Group revealed a set of west-vergent, mesoscale, shallowly north- or south-plunging folds termed D5, similar to the 'Early' folds observed at Ollaberry. The presence of similar folds elsewhere in the Queyfirth Group suggests that the 'Early' folds are regional structures rather than being specifically related to deformation along the WBF (Pringle 1970). Although no geochronology has been carried out in the Queyfirth Group, Rb–Sr mineral age dating within the correlative East Mainland Succession east of the WBF obtained a 480–470 Ma age for the dominant steep ductile fabric (Walker *et al.* 2016). This date suggests a Mid-Ordovician (Grampian) age for the 'Proto' and 'Early' fold and fabric development at Ollaberry.

Watts *et al.* (2007) concluded that the WBF initiated as a strike-slip sinistral fault prior to intrusion of the Graven Complex. Given the *c.* 440 Ma age obtained for this pluton by Lancaster *et al.* (2017), this age implies a pre-Early Silurian age for the initiation of the WBF on Shetland. If correct, the WBF would therefore have initiated significantly earlier than the GGF, the earliest movements along which are thought to have occurred in mainland Scotland at *c.* 430–425 Ma (Stewart *et al.* 2001). However, given the rather limited outcrop of the Graven Complex in northern Shetland, the absence of evidence for early sinistral shear may not be conclusive. It is possible that the pluton was post-dated by sinistral shear and that the deformed material was excised during later faulting along the WBF.

Along-strike and to the south of Ollaberry, fault-bounded slivers of sinistrally sheared blastomylonites–mylonites, possibly derived from orthogneisses equivalent to the Uyea Gneiss Complex or Eastern Gneiss, are preserved at Lunnister and other isolated localities (e.g. Seli Voe and Aith). These display textures consistent with deformation under lower amphibolite to upper greenschist conditions (400–500°C, 12–16 km depth; Watts *et al.* 2007). Importantly, two main comparisons may be made between Ollaberry and Lunnister. First, no regional west-verging folds similar to the 'Early' deformation at Ollaberry are found folding the mylonites at Lunnister. It therefore seems most likely that the mylonites formed later than the inferred Ordovician 'Early' deformation seen at Ollaberry and elsewhere in the Queyfirth Group, although this cannot be proved because all the exposed contacts between the two rock types are faults (Watts *et al.* 2007). Second, almost no sinistral deformation is preserved in the WBF damage zone or adjacent Queyfirth Group at Lunnister or at Ollaberry. Watts *et al.* (2007) suggested that most of the evidence of sinistral movement along the WBF must have been destroyed by post-Caledonian movements and that the sinistral mylonites at Lunnister were exhumed on a restraining bend. Direct dating of the WBF blastomylonites–mylonites at Lunnister is required to unambiguously constrain the age of the initiation of the WBF and to assess the importance of these mylonites in the evolution of the WBF.

Dextral reactivation of the WBF is constrained as being between post-370 Ma (the intrusion age of the Sandsting Granite) and *c.* 330–300 Ma (the likely age of the overlying Permian unconformity offshore) (Watts *et al.* 2007; Lancaster *et al.* 2017). Watts *et al.* (2007) suggested that a Late Carboniferous age for dextral reactivation is most likely based on the recognition of inversion

events in the Orcadian Basin in Orkney and similar fault movements of this age along the GGF (Coward *et al.* 1989; Rogers *et al.* 1989; Seranne 1992; Kemp *et al.* 2019; Dichiarante *et al.* 2020). At Lunnister, Watts *et al.* (2007) recognized extensive sequences of cataclasites and fault gouge assemblages related to deformation at *c.* 5–10 km depth under zeolite facies conditions (100–250°C), along with extensive dextrally verging folds. The conditions at Lunnister are consistent with the 'Late' deformation observed at Ollaberry and suggest that the majority of the present day architecture of the WBF formed during the Carboniferous.

Post-Carboniferous, minor amounts of dip-slip and sinistral strike-slip reactivations of the Walls Boundary Fault Zone were associated with an increasing narrowing of the active fault zone and are almost entirely restricted to movements along discrete brittle discontinuities located in the fault core (Watts *et al.* 2007).

Comparison of Shetland and mainland Scotland in the Late Carboniferous

During the Carboniferous, the Devonian Orcadian Basin was widely affected by local inversion-related folding oriented NNE–SSW (Coward *et al.* 1989; Dichiarante *et al.* 2020). Offset markers in the Devonian Orcadian Basin on the Black Isle indicate 30 km of dextral movement on the NE–SW-oriented GGF in mainland Scotland (Fig. 13) (Donovan *et al.* 1976; Rogers *et al.* 1989). K–Ar dating of illites in sheared phyllosilicate gouge from the Sronlairig Fault, a splay of the GGF, has been used to suggest that the Sronglairig Fault initiated in the Late Carboniferous–Permian (Kemp *et al.* 2019). In the West Orkney Basin and the adjacent north coastal region of Scotland, some larger pre-existing north–south-oriented structures, such as the East Scarpa and Brough

Brims Risa faults, were reactivated as reverse faults (Coward *et al.* 1989; Wilson *et al.* 2010; Dichiarante *et al.* 2016, 2020). On a broader regional scale, other NE–SW-oriented Caledonian basement structures throughout southern Scotland and northern England were also seemingly prone to dextral reactivation during the Late Carboniferous, widely distributing the effects of local east–west compressional deformation through the Midland Valley and Northumberland basins (e.g. see Ritchie *et al.* 2003; De Paola *et al.* 2005).

By comparison, on Shetland, the dominant pre-existing faults and tectonic fabrics are steeply dipping north–south, with 60–95 km of dextral motion thought to have been accommodated by the WBF (Astin 1982; Rogers *et al.* 1989) and 16 km on the Nesting Fault (Flinn 1992). Little Carboniferous deformation is recorded outside the WBF and Nesting Fault damage zones (Fig. 13) and it seems likely that the Yell Sound Group and East Mainland Succession, which have a steeply dipping north–south ductile fabric (Flinn 2007; Walker *et al.* 2020), controlled the location of the Walls Boundary and Nesting faults. It also meant that dextral movement and east–west compressional deformation were very strongly localized along these faults in Shetland. We therefore propose that the pre-existing basement architecture ultimately controlled the patterns of Late Carboniferous deformation: highly localized along north–south structures in Shetland, with locally large dextral offsets along faults, or broadly dispersed over a wider region with smaller individual offsets along NE–SW dextral faults in Scotland and northern England (Fig. 13).

Some workers attribute Late Carboniferous dextral shearing in mainland Scotland and Shetland to the far-field effects of the Variscan orogeny in southern Britain (e.g. Seranne 1992), whereas others attribute the east–west compression to the closure of the Ural
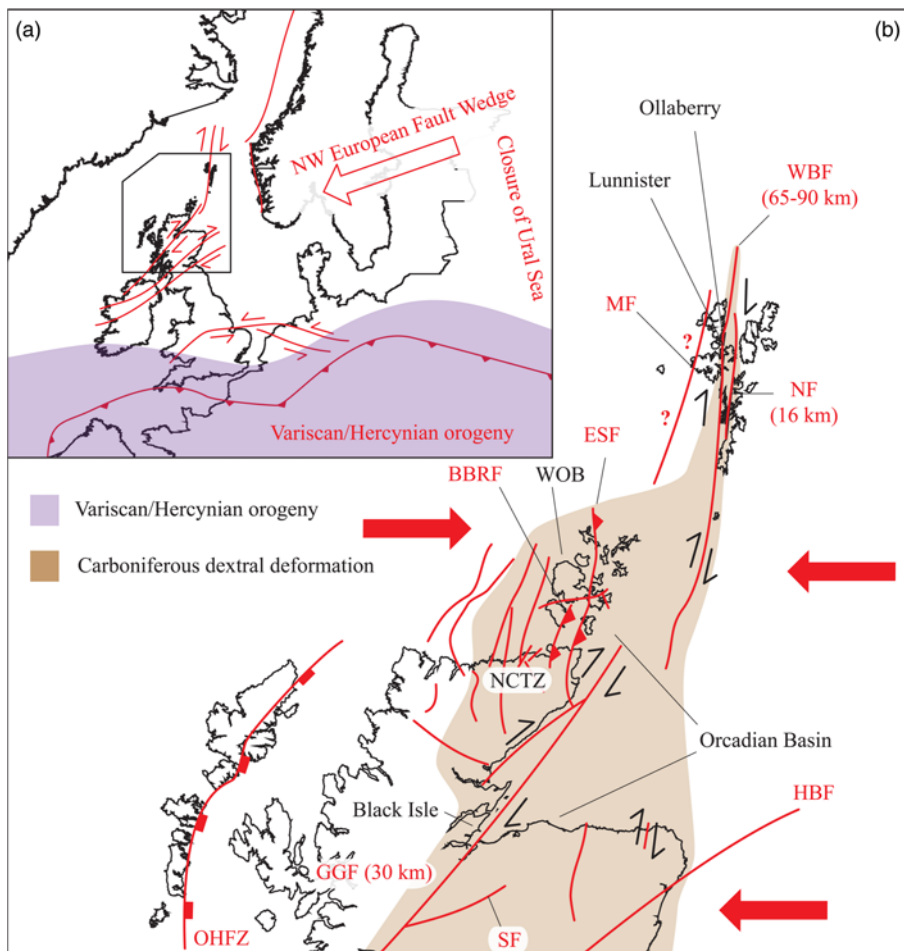
Fig. 13. (**a**) Regional tectonic map of the North Atlantic region during the Late Carboniferous showing the Variscan/Hercynian orogeny to the south of Britain and the westwards movement of the Northern European Fault Block. The Great Glen, Nesting and Walls Boundary faults are restored to their Late Carboniferous positions. (**b**) Local tectonic map of Shetland and northern mainland Scotland showing the main faults active during the Late Carboniferous. Notable faults are labelled in red, whereas the regions and basins are labelled in black. BBRF, Brough Brims Risa Fault; ESF, East Scarpa Fault; GGF, Great Glen Fault; HBF, Highland Boundary Fault; MF, Melby Fault; NCTZ, North Coast Transfer Zone; NF, Nesting Fault; OHFZ, Outer Hebrides Fault Zone; SF, Sronlairig Fault; WBF, Walls Boundary Fault; WOB, West Orkney Basin.

Sea, which caused a NW European fault wedge to be pushed westwards (Bénard *et al.* 1990; Coward 1993; Rey *et al.* 1997) (Fig. 13). According to the fault wedge model, NW European movement is accommodated along sinistral faults (e.g. the Brabant–North Sea fault system in England) and dextral movement on structures such as the GGF and Midland Valley Fault in mainland Scotland (Coward 1993). Our observations show that east–west inversion and dextral strike-slip are coeval in Shetland and are probably related to a dextrally transpressive strain regime associated with the WBF and may be explained either by regional oblique tectonic interactions or the Shetland Platform lying on a restraining bend on the WBF. Invoking a transpressional model removes the need to attribute inversion and dextral deformation to different tectonic events and suggests that existing regional models of Carboniferous–Permian inversion need to be reassessed. More generally, this proposal is consistent with the proposed linking of Late Carboniferous inversion events in Scotland and Orkney in an east–west compressive stress regime (e.g. Wilson *et al.* 2010; Dichiarante *et al.* 2020).

Conclusions

The WBF at Ollaberry juxtaposes rocks belonging to the metasedimentary Precambrian–Cambrian Queyfirth Group against the early Silurian granitic Graven Complex. A highly heterogeneous assemblage of kinematically and geometrically differing 'Early' and 'Late' structures is preserved. In the Queyfirth Group, the 'Early' structures are characterized by mesoscale, tight to isoclinal, west-verging folds thought to have formed as regional structures during the Caledonian Grampian orogeny. Superimposed on the regional structures are 'Late' dextrally verging folds and faults thought to have formed contemporaneously with top-to-the-west reverse faults in both the Queyfirth Group and Graven Complex. These are related to the partitioning of transpressional deformation into domainal reverse dextral strike-slip monoclinic systems and are associated with right-lateral movements along the WBF. On a smaller scale, strain during the 'Late' dextral transpressional event is focused in phyllosilicate-rich pelite layers and reactivates favourably aligned pre-existing structures such as 'Early' fold limbs. In addition, the intensity of 'Late' shearing and the frequency of 'Late' structures progressively increases towards the WBF, culminating in a mélange of flattened quartzite blocks floating in a highly sheared phyllosilicate-rich matrix proximal to the fault. Pre-existing structures and lithological heterogeneity can therefore be important factors in controlling the localization of shortening and wrench partitioning during oblique deformation.

A Late Carboniferous age is most likely for 'Late' deformation and we suggest that contemporaneous east–west compressive and dextral structures on Shetland during this time may be the result of the kinematic partitioning of bulk wrench and reverse monoclinic strain. Regionally, dextral deformation in Shetland was focused on the WBF and the Nesting Fault, unlike in mainland Scotland, which saw a broader, regional-scale distribution of deformation in reactivated faults and folding in pre-existing Devonian basins.

Author contributions **TBA**: conceptualization (equal), formal analysis (lead), investigation (lead), methodology (lead), writing – original draft (lead), writing – review and editing (equal); **LMW**: conceptualization (equal), investigation (equal), methodology (equal); **REH**: conceptualization (lead), investigation (equal), project administration (lead), supervision (lead), writing – original draft (equal), writing – review and editing (equal); **RAS**:

conceptualization (equal), project administration (equal), supervision (equal), writing – original draft (equal), writing – review and editing (equal).

Data availability All data generated or analysed during this study are included in this published article.

Scientific editing by Deta Gasser

References

Andrews, I. 1985. The deep structure of the Moine Thrust, southwest of Shetland. *Scottish Journal of Geology*, **21**, 213–217, https://doi.org/10.1080/1023624021000019333

Astin, T.R. 1982. The Devonian geology of the Walls peninsula, Shetland. PhD thesis, University of Cambridge.

Bénard, F., Mascle, A., Le Gall, B., Doligez, B. and Rossi, T. 1990. Palaeo-stress fields in the Variscan foreland during the Carboniferous from microstructural analysis in the British Isles. *Tectonophysics*, **177**, 1–13, https://doi.org/10.1016/0040-1951(90)90271-9

Clegg, P. and Holdsworth, R.E. 2005. Complex deformation as a result of strain partitioning in transpression zones: an example from the Leinster Terrane, SE Ireland. *Journal of the Geological Society, London*, **162**, 187–202, https://doi.org/10.1144/0016-764903-177

Coward, M.P. 1993. The effect of Late Caledonian and Variscan continental escape tectonics on basement structure, Paleozoic basin kinematics and subsequent Mesozoic basin development in NW Europe. *Geological Society, London, Petroleum Geology Conference Series*, **4**, 1095–1108, https://doi.org/10.1144/0041095

Coward, M.P., Enfield, M.A. and Fischer, M.W. 1989. Devonian basins of Northern Scotland: extension and inversion related to Late Caledonian–Variscan tectonics. *Geological Society, London, Special Publications*, **44**, 275–308, https://doi.org/10.1144/GSL.SP.1989.044.01.16

Crowley, Q.G. and Strachan, R.A. 2015. U-Pb zircon constraints on obduction initiation of the Unst Ophiolite: an oceanic core complex in the Scottish Caledonides? *Journal of the Geological Society, London*, **172**, 279–282, https://doi.org/10.1144/jgs2014-125

Cutts, K.A., Hand, M., Kelsey, D.E., Wade, B., Strachan, R.A., Clark, C. and Netting, A. 2009. Evidence for 930 Ma metamorphism in the Shetland Islands, Scottish Caledonides: implications for Neoproterozoic tectonics in the Laurentia–Baltica sector of Rodinia. *Journal of the Geological Society, London*, **166**, 1033–1047, https://doi.org/10.1144/0016-76492009-006

Cutts, K.A., Hand, M., Kelsey, D.E. and Strachan, R.A. 2011. P-T constraints and timing of Barrovian metamorphism in the Shetland Islands, Scottish Caledonides: implications for the structural setting of the Unst ophiolite. *Journal of the Geological Society, London*, **168**, 1265–1284, https://doi.org/10.1144/0016-76492010-165

De Paola, N., Holdsworth, R.E., McCaffrey, K.J.W. and Barchi, M.R. 2005. Partitioned transtension: an alternative to basin inversion models. *Journal of Structural Geology*, **27**, 607–625, https://doi.org/10.1016/j.jsg.2005.01.006

Dewey, J.F. and Strachan, R.A. 2003. Changing Silurian-Devonian relative plate motion in the Caledonides: sinistral transpression to sinistral transtension. *Journal of the Geological Society, London*, **160**, 219–229, https://doi.org/10.1144/0016-764902-085

Dewey, J.F., Holdsworth, R.E. and Strachan, R.A. 1998. Transpression and transtension zones. *Geological Society, London, Special Publications*, **135**, 1–14, https://doi.org/10.1144/GSL.SP.1998.135.01.01

Dichiarante, A.M., Holdsworth, R.E. *et al.* 2016. New structural and Re–Os geochronological evidence constraining the age of faulting and associated mineralization in the Devonian Orcadian Basin, Scotland. *Journal of the Geological Society, London*, **173**, 457–473, https://doi.org/10.1144/jgs2015-118

Dichiarante, A.M., McCaffrey, K.J., Holdsworth, R.E., Bjornarå, T.I. and Dempsey, E.D. 2020. Fracture attribute scaling and connectivity in the Devonian Orcadian Basin with implications for geologically equivalent sub-surface fractured reservoirs. *Solid Earth Discussions*, 1–48, https://doi.org/10.5194/se-2020-15

Donovan, R.N., Archer, R., Turner, P. and Tarling, D.H. 1976. Devonian palaeogeography of the Orcadian basin and the Great Glen fault. *Nature*, **259**, 550–551, https://doi.org/10.1038/259550a0

Duindam, P. and Van Hoorn, B. 1987. Structural evolution of the West Shetland continental margin. *In: Conference on petroleum geology of North West Europe*. **3**, 765–773.

Ellero, A., Ottria, G., Marroni, M., Pandolfi, L. and Göncüoğlu, M.C. 2015. Analysis of the North Anatolian Shear Zone in Central Pontides (northern Turkey): insight for geometries and kinematics of deformation structures in a transpressional zone. *Journal of Structural Geology*, **72**, 124–141, https://doi.org/10.1016/j.jsg.2014.12.003

Evans, B., Renner, J. and Hirth, G. 2001. A few remarks on the kinetics of static grain growth in rocks. *International Journal of Earth Sciences*, **90**, 88–103, https://doi.org/10.1007/s005310000150

Flinn, D. 1961. Continuation of the Great Glen Fault beyond the Moray Firth. *Nature*, **191**, 589–591, https://doi.org/10.1038/191589b0

Flinn, D. 1977. Transcurrent faults and associated cataclasis in Shetland. *Journal of the Geological Society, London*, **133**, 231–247, https://doi.org/10.1144/gsjgs.133.3.0231

Flinn, D. 1988. The Moine rocks of Shetland. *In*: Winchester, J.A. (ed.) *Later Proterozoic Stratigraphy of the Northern Atlantic Regions*. Blackie, Glasgow, 74–85.

Flinn, D. 1992. The history of the Walls Boundary fault, Shetland: the northward continuation of the Great Glen fault from Scotland. *Journal of the Geological Society, London*, **149**, 721–726, https://doi.org/10.1144/gsjgs.149.5.0721

Flinn, D. 1999. The architecture of the Shetland Ophiolite. *Scottish Journal of Geology*, **36**, 123–135, https://doi.org/10.1144/sjg36020123

Flinn, D. 2001. The basic rock of the Shetland Ophiolite Complex and their bearing of its genesis. *Scottish Journal of Geology*, **37**, 79–96, https://doi.org/10.1144/sjg37020079

Flinn, D. 2007. The Dalradian rocks of Shetland and their implications for the plate tectonics of the northern Iapetus. *Scottish Journal of Geology*, **43**, 125–142, https://doi.org/10.1144/sjg43020125

Flinn, D., Frank, P.L., Brook, M. and Pringle, I.R. 1979. Basement–cover relations in Shetland. *Geological Society, London, Special Publications*, **8**, 109–115, https://doi.org/10.1144/GSL.SP.1979.008.01.09

Fossen, H. and Tikoff, B. 1997. Forward modelling of non-steady-state deformations and the 'minimum strain path'. *Journal of Structural Geology*, **19**, 987–996, https://doi.org/10.1016/S0191-8141(97)00021-7

Fossen, H. and Tikoff, B. 1998. Extended models of transpression and transtension, and application to tectonic settings. *Geological Society, London, Special Publications*, **135**, 15–33, https://doi.org/10.1144/GSL.SP.1998.135.01.02

Harland, W.B. 1971. Tectonic transpression in Caledonian Spitsbergen. *Geological Magazine*, **108**, 27–41, https://doi.org/10.1017/S0016756800050937

Hirth, G. and Tullis, J. 1992. Dislocation creep regimes in quartz aggregates. *Journal of Structural Geology*, **14**, 145–159, https://doi.org/10.1016/0191-8141(92)90053-Y

Holdsworth, R.E., Tavarnelli, E. and Clegg, P. 2002. The nature and regional significance of structures in the Gala group of the Southerns Uplands terrane, Berwickshire coast, southeastern Scotland. *Geological Magazine*, **139**, 707–717, https://doi.org/10.1017/S0016756802006854

Holdsworth, R.E., Morton, A. *et al.* 2019. The nature and significance of the Faroe-Shetland Terrane: linking Archaean basement blocks across the North Atlantic. *Precambrian Research*, **321**, 154–171, https://doi.org/10.1016/j.precamres.2018.12.004

Jones, R.R. and Holdsworth, R.E. 1998. Oblique simple shear in transpression zones. *Geological Society, London, Special Publications*, **135**, 35–40. https://doi.org/10.1144/GSL.SP.1998.135.01.03.

Jones, R.R., Holdsworth, R.E. and Bailey, W. 1997. Lateral extrusion in transpression zones: the importance of boundary conditions. *Journal of Structural Geology*, **19**, 1201–1217, https://doi.org/10.1016/S0191-8141(97)00034-5

Jones, S.M., White, N., Clarke, B.J., Rowley, E. and Gallagher, K. 2002. Present and past influence of the Iceland plume on sedimentation. *Geological Society, London, Special Publications*, **196**, 13–25. https://doi.org/10.1144/GSL.SP.2002.196.01.02.

Jones, R.R., Holdsworth, R.E., Clegg, P., McCaffrey, K. and Tavarnelli, E. 2004. Inclined transpression. *Journal of Structural Geology*, **26**, 1531–1548, https://doi.org/10.1016/j.jsg.2004.01.004

Jones, R.R., Holdsworth, R.E., McCaffrey, K.J.W., Clegg, P. and Tavarnelli, E. 2005. Scale dependence, strain compatibility and heterogeneity of three-dimensional deformation during mountain building: a discussion. *Journal of Structural Geology*, **27**, 1190–1204, https://doi.org/10.1016/j.jsg.2005.04.001

Kemp, S.J., Gillespie, M.R., Leslie, G.A., Zwingmann, H. and Campbell, S.D.G. 2019. Clay mineral dating of displacement on the Sronlairig Fault: implications for Mesozoic and Cenozoic tectonic evolution in northern Scotland. *Clay Minerals*, 1–63, https://doi.org/10.1180/clm.2019.25

Kinny, P.D., Strachan, R.A. *et al.* 2019. The Neoarchean Uyea Gneiss Complex, Shetland: an onshore fragment of the Rae Craton on the European plate. *Journal of the Geological Society, London*, **176**, 847–862, https://doi.org/10.1144/jgs2019-017.

Kruhl, J.H. 1998. Reply: prism- and basal-plane parallel sub- grain boundaries in quartz: a microstructural geothermobarometer. *Journal of Metamorphic Geology*, **16**, 142–146.

Lancaster, P.J., Strachan, R.A., Bullen, D., Fowler, M., Jaramillo, M. and Saldarriaga, A.M. 2017. U–Pb zircon geochronology and geodynamic significance of 'Newer Granite' plutons in Shetland, northernmost Scottish Caledonides. *Journal of the Geological Society, London*, **174**, 486–497, https://doi.org/10.1144/jgs2016-106

Le Breton, E., Cobbold, P.R. and Zanella, A. 2013. Cenozoic reactivation of the Great Glen Fault, Scotland: additional evidence and possible causes. *Journal of the Geological Society, London*, **170**, 403–415, https://doi.org/10.1144/jgs2012-067

McBride, J.H. 1994. Investigating the crustal structure of a strike-slip "step-over" zone along the Great Glen fault. *Tectonics*, **13**, 1150–1160, https://doi.org/10.1029/94TC00539

McBride, J.H. and England, R.W. 1994. Deep seismic reflection structure of the Caledonian orogenic front west of Shetland. *Journal of the Geological Society, London*, **151**, 9–16, https://doi.org/10.1144/gsjgs.151.1.0009

McCaffrey, K.J.W., Jones, R.R. *et al.* 2005. Unlocking the spatial dimension: digital technologies and the future of geoscience fieldwork. *Journal of the Geological Society, London*, **162**, 927–938, https://doi.org/10.1144/0016-764905-017

McGeary, S. 1989. Reflection seismic evidence for a Moho offset beneath the Walls Boundary strike-slip fault. *Journal of the Geological Society, London*, **146**, 261–269, https://doi.org/10.1144/gsjgs.146.2.0261

Mykura, W. 1976. *British Regional Geology: Orkney and Shetland*. HMSO, Edinburgh.

Mykura, W. and Phemister, J. 1976. *The Geology of Western Shetland*. Memoir of the Geological Survey, Great Britain.

Passchier, C.W. and Trouw, R.A. 2005. *Microtectonics*. Springer Science & Business Media.

Prave, A.R., Strachan, R.A. and Fallick, A.E. 2009. Global C cycle perturbations recorded in marbles: a record of Neoproterozoic Earth history within the Dalradian succession of the Shetland Islands, Scotland. *Journal of the Geological Society, London*, **166**, 129–135, https://doi.org/10.1144/0016-76492007-126

Pringle, I.R. 1970. The structural geology of the North Roe area of Shetland. *Geological Journal*, **7**, 147–170, https://doi.org/10.1002/gj.3350070109

Ramsay, J.G. 1967. *Folding and Fracturing of Rocks*. McGraw-Hill, New York.

Rey, P., Burg, J.-P. and Casey, M. 1997. The Scandinavian Caledonides and their relationship to the Variscan belt. *Geological Society, London, Special Publications*, **121**, 179–200, https://doi.org/10.1144/GSL.SP.1997.121.01.08

Richards, P.C. 1990. The early to mid-Jurassic evolution of the northern North Sea. *Geological Society, London, Special Publications*, **55**, 191–205, https://doi.org/10.1144/GSL.SP.1990.055.01.09

Ritchie, J.D., Johnson, H., Browne, M.A.E. and Monaghan, A.A. 2003. Late Devonian-Carboniferous tectonic evolution within the Firth of Forth, Midland Valley: as revealed from 2D seismic reflection data. *Scottish Journal of Geology*, **39**, 121–134, https://doi.org/10.1144/sjg39020121

Ritchie, J., Johnson, H, Kimbell, G. & Quinn, M. 2013. Structure. *In*: Hitchen, K., Johnson, H. & Gatliff, R.W. (eds) *Geology of the Rockall Basin and Adjacent Areas*. British Geological Survey, London, Research Report RR/12/03, 10–46.

Rogers, D.A., Marshall, J.E.A. and Astin, T.R. 1989. Devonian and later movements on the Great Glen Fault system, Scotland. *Journal of the Geological Society, London*, **146**, 369–372, https://doi.org/10.1144/gsjgs.146.3.0369

Rutter, E.H. 1983. Pressure solution in nature, theory and experiment. *Journal of the Geological Society, London*, **140**, 725–740, https://doi.org/10.1144/gsjgs.140.5.0725

Ryan, P.D. and Dewey, J.F. 1991. A geological and tectonic cross-section of the Caledonides of western Ireland. *Journal of the Geological Society, London*, **148**, 173–180, https://doi.org/10.1144/gsjgs.148.1.0173

Sanderson, D.J. and Marchini, W.R.D. 1984. Transpression. *Journal of Structural Geology*, **6**, 449–458, https://doi.org/10.1016/0191-8141(84)90058-0

Seranne, M. 1992. Devonian extensional tectonics versus Carboniferous inversion in the northern Orcadian basin. *Journal of the Geological Society, London*, **149**, 27–37, https://doi.org/10.1144/gsjgs.149.1.0027

Spray, J.G. 1988. Thrust-related metamorphism beneath the Shetland Islands oceanic fragment, northeast Scotland. *Canadian Journal of Earth Sciences*, **25**, 1760–1776, https://doi.org/10.1139/e88-167

Spray, J.G. and Dunning, G.R. 1991. A U/Pb age for the Shetland Islands oceanic fragment, Scottish Caledonides: evidence from anatectic plagiogranites in 'layer 3' shear zones. *Geological Magazine*, **128**, 667–671, https://doi.org/10.1017/S0016756800019762

Stewart, M., Strachan, R.A. and Holdsworth, R.E. 1999. Structure and early kinematic history of the Great Glen Fault Zone, Scotland. *Tectonics*, **18**, 326–342, https://doi.org/10.1029/1998TC900033

Stewart, M., Strachan, R.A., Martin, M.W. and Holdsworth, R.E. 2001. Constraints on early sinistral displacements along the Great Glen Fault Zone, Scotland: structural setting, U-Pb geochronology and emplacement of the syn-tectonic Clunes tonalite. *Journal of the Geological Society, London*, **158**, 821–830, https://doi.org/10.1144/jgs.158.5.821

Stipp, M., Stünitz, H., Heilbronner, R. and Schmid, S.M. 2002. The eastern Tonale fault zone: a 'natural laboratory' for crystal plastic deformation of quartz over a temperature range from 250 to 700°C. *Journal of Structural Geology*, **24**, 1861–1884, https://doi.org/10.1016/S0191-8141(02)00035-4

Strachan, R.A., Prave, A.R., Kirkland, C.L. and Storey, C.D. 2013. U–Pb detrital zircon geochronology of the Dalradian Supergroup, Shetland Islands, Scotland: implications for regional correlations and Neoproterozoic–Palaeozoic basin development. *Journal of the Geological Society, London*, **170**, 905–916, https://doi.org/10.1144/jgs2013-057

Tavarnelli, E. 1998. Tectonic evolution of the Northern Salinian Block, California, USA: Paleogene to Recent shortening in a transform fault-bounded continental fragment. *Geological Society, London, Special Publications*, **135**, 107–118, https://doi.org/10.1144/GSL.SP.1998.135.01.07

Tavarnelli, E. and Holdsworth, R.E. 1999. How long do structures take to form in transpression zones? A cautionary tale from California. *Geology*, **27**, 1063–1066, https://doi.org/10.1130/0091-7613(1999)027<1063:HLDSTT>2.3.CO;2

Tavarnelli, E., Holdsworth, R.E., Clegg, P., Jones, R.R. and McCaffrey, K.J.W. 2004. The anatomy and evolution of a transpressional imbricate zone, Southern Uplands, Scotland. *Journal of Structural Geology*, **26**, 1341–1360, https://doi.org/10.1016/j.jsg.2004.01.003

ten Grotenhuis, S.M., Trouw, R.A.J. and Passchier, C.W. 2003. Evolution of mica fish in mylonitic rocks. *Tectonophysics*, **372**, 1–21, https://doi.org/10.1016/S0040-1951(03)00231-2

Teyssier, C. and Tikoff, B. 1998. Strike-slip partitioned transpression of the San Andreas fault system: a lithospheric-scale approach. *Geological Society, London, Special Publications*, **135**, 143–158, https://doi.org/10.1144/GSL.SP.1998.135.01.10

Teyssier, C., Tikoff, B. and Markley, M. 1995. Oblique plate motion and continental tectonics. *Geology*, **23**, 447–450, https://doi.org/10.1130/0091-7613(1995)023<0447:OPMACT>2.3.CO;2

Tikoff, B. and Fossen, H. 1993. Simultaneous pure and simple shear: the unifying deformation matrix. *Tectonophysics*, **217**, 267–283, https://doi.org/10.1016/0040-1951(93)90010-H

Tikoff, B. and Teyssier, C. 1994. Strain modeling of displacement-field partitioning in transpressional orogens. *Journal of Structural Geology*, **16**, 1575–1588, https://doi.org/10.1016/0191-8141(94)90034-5

Walker, S., Thirlwall, M.F., Strachan, R.A. and Bird, A.F. 2016. Evidence from Rb–Sr mineral ages for multiple orogenic events in the Caledonides of Shetland, Scotland. *Journal of the Geological Society, London*, **173**, 489–503, https://doi.org/10.1144/jgs2015-034

Walker, S., Bird, A.F., Thirlwall, M.F. and Strachan, R.A. 2020. Caledonian and pre-Caledonian orogenic events in Shetland, Scotland: evidence from garnet Lu-Hf and Sm-Nd geochronology. *In*: Murphy, J.B., Strachan, R.A. and Quesada, C. (eds) *Pannotia to Pangaea: Neoproterozoic and Paleozoic Orogenic Cycles in the Circum-Atlantic Region*. Geological Society, London, Special Publications, **503**, first published online September 14, 2020, https://doi.org/10.1144/SP503-2020-32

Watts, L.M., Holdsworth, R.E., Sleight, J.A., Strachan, R.A. and Smith, S.A.F. 2007. The movement history and fault rock evolution of a reactivated crustal-scale strike-slip fault: the Walls Boundary Fault Zone, Shetland. *Journal of the Geological Society, London*, **164**, 1037–1058, https://doi.org/10.1144/0016-76492006-156

Wilson, R.W., Holdsworth, R.E., Wild, L.E., McCaffrey, K.J.W., England, R.W., Imber, J. and Strachan, R.A. 2010. Basement-influenced rifting and basin development: a reappraisal of post-Caledonian faulting patterns from the North Coast Transfer Zone, Scotland. *Geological Society, London, Special Publications*, **335**, 795–826, https://doi.org/10.1144/SP335.32